

**Lattice study of pentaquark states**C. Alexandrou<sup>1</sup> and A. Tsapalis<sup>1,2</sup><sup>1</sup>*Department of Physics, University of Cyprus, CY-1678 Nicosia, Cyprus*<sup>2</sup>*Institute of Accelerating Systems and Applications, University of Athens, Athens, Greece*

(Received 13 March 2005; revised manuscript received 12 September 2005; published 17 January 2006)

We present a study of the pentaquark system in quenched lattice QCD using diquark-diquark and kaon-nucleon local and smeared interpolating fields. We examine the volume dependence of the spectral weights of local correlators on lattices of size  $16^3 \times 32$ ,  $24^3 \times 32$ , and  $32^3 \times 64$  at  $\beta = 6.0$ . We find that a reliable evaluation of the volume dependence of the spectral weights requires accurate determination of the correlators at large time separations. Our main result from the spectral weight analysis in the pentaquark system is that within our variational basis and statistics we cannot exclude a pentaquark resonance. However, our data also do not allow a clear identification of a pentaquark state since only the spectral weights of the lowest state can be determined to sufficient accuracy to test for volume dependence. In the negative parity channel, the mass extracted for this state is very close to the kaon-nucleon threshold, whereas in the positive parity channel it is about 60% above.

DOI: [10.1103/PhysRevD.73.014507](https://doi.org/10.1103/PhysRevD.73.014507)

PACS numbers: 11.15.Ha, 12.38.Gc, 12.38.Aw, 12.38.-t

**I. INTRODUCTION**

Experimental searches for a pentaquark state near the kaon-nucleon (KN) threshold, reported in recent experiments [1,2], are under way worldwide. The accumulation of evidence from low energy experiments for the existence of this state [3] combined with the negative results obtained in high energy experiments [4] pose deep questions as to its nature and its production mechanism. Further doubts as to the existence of the  $\Theta^+$  have been raised by the recent report of the CLAS collaboration claiming lack of evidence for a resonance state from a dedicated high statistics proton experiment [5]. The  $\Theta^+$  was predicted theoretically in the chiral soliton model [6] as an exotic baryon state with an unusually narrow width. The possible existence of such a state has raised interesting questions on what its structure should be in order to account for its narrow width. A number of phenomenological models have been put forward to explain its stability such as special flux tube configurations [7–10] and diquark formation [11].

Several studies in lattice QCD have looked for a pentaquark state in order to determine its mass and parity but no consensus has been reached yet with some groups finding a bound state with mass close to the experimental value [12,14,13,15,16] and others the KN scattering state [17–19]. One main difference between these groups has been the interpolating field used to create this state [20]. Since its structure is unknown, optimizing the interpolating field that one uses is a difficult task. However, for reasonable interpolating fields, the results should not be dependent on the interpolating field. In this work we use two of the most popular choices: an interpolating field motivated by the diquark-diquark picture [11] and an interpolating field motivated by the kaon-nucleon structure [8]. We note that diquark formation was shown to be important in the context of the static pentaquark potential where arrange-

ments of quarks that allow diquark formation are found to be energetically favored giving rise to a potential that is proportional to the minimal flux tube connecting the five quarks [10,15,21]. Using these interpolating fields as a basis, we construct a  $2 \times 2$  mass correlation matrix and determine the optimal linear combination that yields maximum overlap with the ground state of the system. Another way of enhancing the ground state by suppressing excited state contributions is smearing. In addition to using local interpolating fields, we also use smeared fields by applying gauge invariant smearing to the quark fields used. We find that the value we obtain for the mass is independent of which of these various interpolating fields we use. Since both interpolating fields have an overlap with the KN scattering state we expect, that being the lowest state, it will determine the large time dependence of both correlators. If a pentaquark bound state exists about 100 MeV higher than the KN threshold, we expect it to dominate the time dependence of the correlator up to time separations of about  $\sim 10 \text{ GeV}^{-1}$ . Therefore the main difficulty is to identify unambiguously the resonance in an intermediate time range before the nearby KN scattering state dominates. If our interpolating fields have good overlap with the KN scattering state and the  $\Theta^+$ , then diagonalization of the mass correlation matrix should give as lowest eigenvalues these two states. This is our motivation for choosing the KN-interpolating field, which is expected to have large overlap with the KN scattering states and the diquark-diquark field expected to have large enough overlap with the pentaquark state. To distinguish a single particle state from a scattering state, the tools that we have at our disposal are the volume dependence of the energy and spectral weights of the state, provided we can isolate it with sufficient accuracy. The energy of a scattering state on a lattice, with the exception of s-wave scattering states, is volume dependent. This is because, in the center of mass frame, the two particles have nonzero relative momentum,

which on a finite lattice depends on the spatial size of the lattice. This means that if a scattering state with nonzero momentum dominates the correlator then its energy will depend on the spatial length of the lattice. The other criterion that can be used is the scaling of the spectral weights with the spatial volume. For a two-particle scattering state the spectral weights are expected to be inversely proportional to the spatial volume, whereas for a resonance there should be no volume dependence. The spectral decomposition of the correlator was given by Lüscher [22], who first noted that a weakly interacting two-particle state well below resonance energy should contribute to the correlator with an amplitude that scales inversely proportional to the volume. The scaling of the spectral weights as a probe for a two-particle resonance scattering state was first used in a lattice study of the pentaquark system by Mathur *et al.* [17]. In order to check how reliably we can extract the scaling of spectral weights in practice, we study the two-pion system in the isospin  $I = 2$  channel for which no low energy resonances are present. This study is done on three lattices of size  $16^3 \times 32$ ,  $24^3 \times 32$ , and  $32^3 \times 64$  at  $\beta = 6.0$ , which are the same lattices used in the study of the pentaquark system. We consider four different two-pion interpolating fields and determine accurately the two lowest energy eigenstates. What we find is that the value of spectral weights extracted stabilizes only at large enough time separations and only then the ratio of spectral weights reaches the expected value. Therefore to check for volume dependence one requires very accurate data so that the extracted ratio of spectral weights is precise enough. For the two-pion system, given our statistics, this can only be achieved for the lowest eigenstate. How large contributions from higher relative momentum states are can be assessed by explicitly projecting to zero relative momentum. This is done for the lattice of size  $16^3 \times 32$  and the results obtained are compared to those without explicit projection to zero relative momentum. We note that such a comparison has not been carried out in previous lattice studies of the pentaquark system. We confirm that diagonalization of the correlation matrix without explicit projection yields a lowest energy eigenvalue that contains contributions from states with higher momenta and only becomes a pure s-wave scattering state at large time separations. This means that in order to obtain the lowest scattering state one must allow for larger time separation as the spatial extent of the lattice increases. As we will demonstrate for a lattice of spatial size of 3 fm, one has to go beyond a time interval of  $30a \sim 15 \text{ GeV}^{-1}$  to obtain the lowest scattering state. This is why we use Dirichlet boundary conditions (b.c.) in the temporal direction. In the study of the two-pion system, we use the heaviest pion mass considered in this work, namely  $\kappa_l = 0.153$ , to have the smallest statistical errors. We compare the scaling behavior of spectral weights in the two-pion and pentaquark system using the same value of  $\kappa_l$ . Our

main conclusion is that, within the accuracy that the spectral weights can be determined from our data, we cannot exclude a pentaquark resonance. In the negative parity channel within our variational basis, we only obtain the lowest eigenstate accurately enough to be able to perform the scaling analysis of the spectral weights. Because of this we are unable to draw a definite conclusion regarding the existence of the  $\Theta^+$ . For the positive parity channel, we obtain two eigenstates very close in energy which at the two heaviest light quark masses have an energy gap of about 100 MeV independent of the spatial volume. It becomes more difficult to obtain an accurate determination for this energy gap as the quark mass gets lighter. Although we find an energy gap that is of the right order, the mass for this state is high: Measuring the mass in the positive parity channel for five values of light quark masses on our largest lattice using a smeared diquark-diquark interpolating field for the source and a local one for the sink and extrapolating to the chiral limit, we obtain a value of  $1.65 \pm 0.09$  times the mass of the noninteracting KN state. This value is too high to be identified with the  $\Theta^+(1540)$ . The values of the light quark mass that we use in carrying out the extrapolation correspond to pion masses in the range of about 900–420 MeV.

## II. LATTICE TECHNIQUES

In this work we consider two interpolating fields motivated by recent proposals on the possible structure of the  $\Theta^+$  state. The first is based on the idea of diquark formation [11] and the other on a diquark-triquark structure [8]. Both have been used in previous lattice studies but a correlation matrix analysis in the manner considered here has not been presented. We will refer to the first as diquark-diquark interpolating field. It is given by

$$J_{DD} = \epsilon^{abc} \epsilon^{aef} \epsilon^{bgh} C \bar{s}_c^T (u_e^T C d_f) (u_g^T C \gamma_5 d_h), \quad (1)$$

where  $C = \gamma_0 \gamma_2$  is the charge conjugation operator. It was first proposed and used in the study of the pentaquark system on the lattice by Sasaki [13]. After performing the antisymmetric tensor contraction, we generalize the resulting expression to obtain an isospin  $I = 0$  and  $I = 1$  interpolating fields:

$$J_{DD} = \epsilon^{abc} (u_a^T C \gamma_5 d_b) [(u_c^T C d_e) \mp (u_e^T C d_c)] C \bar{s}_e^T. \quad (2)$$

The minus sign corresponds to isospin  $I = 0$  and the plus sign to isospin  $I = 1$ . The second field, which we will refer to as the KN-interpolating field, is given by

$$J_{NK} = \epsilon^{abc} (u_a^T C \gamma_5 d_b) [u_c (\bar{s} \gamma_5 d) \mp d_c (\bar{s} \gamma_5 u)], \quad (3)$$

where the minus sign corresponds to the isoscalar and the plus to the isovector. Although we have used both the isoscalar and the isovector interpolating fields, in this work we will only discuss the results in the isospin zero channel.

As presented, the interpolating fields have opposite parities with  $J_{DD}$  having positive parity and  $J_{KN}$  negative. The parity of these fields can be flipped by multiplying with  $\gamma_5$ . The two point correlator can couple both to positive and negative parity states and the propagators for the positive and negative parity interpolating fields are given, respectively, by [23]

$$\begin{aligned} G_+(t) &= \frac{(1 + \gamma_0)}{2} g(t) + \frac{(1 - \gamma_0)}{2} g(-t) \\ G_-(t) &= \frac{(1 - \gamma_0)}{2} g(t) - \frac{(1 + \gamma_0)}{2} g(-t) \\ g(t) &= \theta(t)C_+ e^{-m^+ t} + \theta(-t)C_- e^{-m^- t}, \end{aligned} \quad (4)$$

where  $m^+$  ( $m^-$ ) is the mass of the positive (negative) parity state. Employing Dirichlet boundary conditions means that only the terms with  $t > 0$  contribute and therefore the positive and negative parity states correspond to the upper and lower Dirac components of  $G_+(t)$  or the lower and upper components of  $G_-(t)$ , respectively. For the two smaller volumes we use only Dirichlet b.c. and local interpolating fields since the main purpose of the evaluation on the smaller lattices is to examine the volume dependence of the spectral weights in the correlators. In order to perform our volume studies we also use Dirichlet b.c. for the local interpolating field on our largest volume. However, the  $32^3 \times 64$  lattice has a time extent large enough so that backwards moving quarks are suppressed and antiperiodic boundary conditions can also be used without affecting the identification of the parity. Therefore on the large volume we opt for antiperiodic b.c. when using smeared sources. It is well known that smearing improves the overlap of the interpolating field with the ground state since it produces an extended source of size typical to that of physical hadrons. We perform gauge invariant smearing [24] by replacing a local quark field  $u(x)$  appearing in the interpolating fields by a smeared one,  $\tilde{u}(x)$ , obtained by

$$\tilde{u}(\mathbf{x}, t) = \sum_{\mathbf{y}} \Phi(\mathbf{x}, \mathbf{y}; U(t)) u(\mathbf{y}, t). \quad (5)$$

The gauge invariant smearing function  $\Phi(\mathbf{x}, \mathbf{y}; U(t))$  is given by

$$\Phi(\mathbf{x}, \mathbf{y}; U(t)) = (1 + \alpha H)^n(\mathbf{x}, \mathbf{y}; U(t)) \quad (6)$$

where the hopping matrix  $H$  is defined by

$$H(\mathbf{x}, \mathbf{y}; U(t)) = \sum_{j=1}^3 [U_j(\mathbf{x}, t) \delta_{\mathbf{x}, \mathbf{y}-\hat{j}} + U_j^\dagger(\mathbf{x} - \hat{j}, t) \delta_{\mathbf{x}, \mathbf{y}+\hat{j}}]. \quad (7)$$

The parameters  $\alpha = 4$  and  $n = 50$  are optimized to approximately reproduce the root mean square radius of the nucleon in the quenched theory at  $\beta = 6.0$  where all the computations are carried out.

Having  $M$  interpolating fields, we can construct an  $M \times M$  mass correlation matrix

$$C_{i;j}(t) = \int d^3x \langle 0 | J_i(\mathbf{x}, t) J_j^\dagger(\mathbf{0}, 0) | 0 \rangle, \quad (8)$$

where in the case of the pentaquark system the indices  $i, j = DD$  or  $KN$ . For nonvanishing results we must use interpolating fields of the same parity. This can be easily achieved by multiplying for example  $J_{DD}$  with  $\gamma_5$ . Our variational analysis is performed in two ways: (i) We solve the generalized eigenvalue equation

$$C(t_1)v_n(t_1) = \lambda_n(t_1, t_0)C(t_0)v_n(t_0). \quad (9)$$

For a large time separation  $t_1 - t_0$  the eigenvalues are given by  $\lambda_n(t_1, t_0) = \exp(-E_n(t_1 - t_0))$ ,  $n = 0, 1, \dots, M - 1$ , yielding the energies  $E_n$  of the  $M$  lowest states [25] with total momentum zero. The energy of the  $M$ th eigenstate is usually poorly determined since it has contributions from all the higher excited states, except when our variational basis contains interpolating fields with a sizable overlap with all  $M$  lowest states. In this analysis we take  $t_0/a = 3-6$  with  $a$  the lattice spacing and check that the values that we find for  $E_n$  do not change as we vary  $t_0$ . (ii) We first diagonalize the correlation matrix  $C(t_0)$

$$C(t_0)v_n(t_0) = \lambda_n(t_0)v_n(t_0) \quad (10)$$

to determine the eigenvectors  $v(t_0)$  taking  $t_0/a = 1$ . We use these eigenvectors to project to the space spanned by the  $N \leq M$  largest eigenvalues  $\lambda_n(t_0)$

$$C_{ij}^N(t) = (v_i, C(t)v_j), \quad i, j = 0, \dots, N - 1 \quad (11)$$

and solve the generalized eigenvector equation given in Eq. (9) but for the projected correlation matrix  $C_{ij}^N$  instead of  $C(t)$ . We denote the resulting eigenvalues by  $\Lambda_n$ . The eigenvectors,  $\mathcal{V}_n$ , that we find determine the best linear combination  $\sum_n \mathcal{V}_n J_n$  that has maximum overlap with the  $N$  lowest eigenstates. We will refer to this linear combination as the optimal interpolating field,  $J_{\text{optimal}}$ . The optimal correlator can be obtained by projecting  $C^N$ :  $(\mathcal{V}_i, C^N \mathcal{V}_j)$  which yields the same energies as those extracted from the eigenvalues  $\Lambda_n$ . We check that the eigenvalues,  $\Lambda_n$  that we obtain by diagonalizing  $C_{ij}^N$  are in agreement with  $\lambda_n$ .

For the pentaquark system, in addition, to  $C_{DD;KN}$  constructed using the local interpolating fields  $J_{DD}$  and  $J_{KN}$  as a basis, we also consider  $\tilde{C}_{DD;KN}$  constructed using smeared fields  $\tilde{J}_{DD}$  and  $\tilde{J}_{KN}$  for the source but keeping the sink local and vice versa. The eigenvalues,  $\tilde{\Lambda}_n$ , extracted from this correlation matrix should yield, for large enough time separations, the same energies as those extracted from  $\Lambda_n$ . We check for consistency at the two heaviest light quark masses, namely  $\kappa_l = 0.153$  and  $\kappa_l = 0.155$ .

The contractions needed for the computation of the pentaquark matrix elements are optimized by doing all the Dirac contractions explicitly before summing over color. For example, using the  $J_{DD}$  interpolating field as source and sink, the correlator is given by

$$C_{DD;DD}(t) = \sum_x \epsilon^{a'b'c'} \epsilon^{abc} [-C\gamma_5 S^*(x) C\gamma_5]_{\mu'\mu'}^{f'f} \{ [\text{Tr}(C\gamma_5 D^{c'c}(x) C\gamma_5 U^{b'bT}(x)) \text{Tr}(CD^{f'f}(x) CU^{a'aT}(x)) \\ - \text{Tr}(C\gamma_5 D^{c'f}(x) CU^{b'bT}(x)) \text{Tr}(CD^{f'c}(x) C\gamma_5 U^{a'aT}(x)) + \text{Tr}(C\gamma_5 D^{c'c}(x) C\gamma_5 U^{a'aT}(x) CD^{f'f}(x) CU^{b'ibT}(x)) \\ - \text{Tr}(C\gamma_5 D^{c'f}(x) CU^{a'aT}(x) CD^{f'c}(x) C\gamma_5 U^{b'ibT}(x))] + [a' \leftrightarrow f'; a \leftrightarrow f] - [a' \leftrightarrow f'] - [a \leftrightarrow f] \}, \quad (12)$$

where  $S(x)$ ,  $U(x)$ , and  $D(x)$  denote the strange, up, and down quark propagators, Latin letters denote color indices, Greek letters Dirac indices, and the transpose acts only on Dirac indices. In each of the terms we perform the Dirac algebra separately and store the result in an array; e.g. in the first term having two traces we construct the traces and then we multiply them and sum over color indices. This reduces the time needed by more than an order of magnitude to about twice the time one needs for the nucleon correlator. Such grouping of terms is common in many lattice studies of matrix elements as, for example, in Refs. [17,19,26].

### III. RESULTS

The lattices and values of the hopping parameter,  $\kappa_l$ , that we use for the light quarks are listed in Table I, where we also give the mass of the pion, the kaon, and the nucleon at

TABLE I. In the first column we give the lattice volume and in the second column the value of the hopping parameter,  $\kappa_l$ , for light quarks. In the third, fourth, fifth, and sixth columns, we give the pion mass, the kaon mass, the nucleon mass, and the  $N^*$  mass in lattice units. For  $\kappa_l = 0.1558$  and  $0.1562$ , the mass of  $N^*$  is not given since no clear plateaus could be identified.

Volume	$\kappa_l$	$m_\pi$	$m_K$	$m_N$	$m_{N^*}$
Local source and sink using Dirichlet b.c. and $J_{DD}$ , $J_{KN}$					
$16^3 \times 32$	0.153	0.422(2)	0.363(2)	0.787(8)	1.039(56)
	0.155	0.295(3)	0.295(3)	0.623(14)	0.895(86)
$24^3 \times 32$	0.153	0.426(3)	0.369(2)	0.790(10)	1.026(42)
	0.155	0.302(3)	0.302(2)	0.644(12)	0.877(57)
$32^3 \times 64$	0.153	0.420(2)	0.361(2)	0.788(6)	0.987(33)
	0.155	0.294(2)	0.294(2)	0.633(7)	0.849(46)
Smear source and local sink using antiperiodic b.c. and $J_{DD}$					
$32^3 \times 64$	0.153	0.418(2)	0.358(2)	0.778(6)	0.990(30)
	0.1550	0.292(2)	0.292(2)	0.625(7)	0.802(44)
	0.1554	0.262(2)	0.277(2)	0.590(9)	0.748(49)
	0.1558	0.229(2)	0.262(2)	0.553(9)	
	0.1562	0.192(2)	0.246(2)	0.513(10)	
$\kappa_c = 0.1571$	0	0.207(5)	0.420(10)		
Smear source and sink using antiperiodic b.c. and $J_{DD}$					
$32^3 \times 64$	0.153	0.418(2)	0.360(3)	0.789(9)	0.973(39)

each value of  $\kappa_l$  as well as the value obtained by linear extrapolation to the chiral limit using the form

$$m_H^2 = a + bm_\pi^2. \quad (13)$$

In Eq. (13)  $m_H$  denotes the mass of any of the hadrons considered in this work. In Table I we also include the mass of the negative parity baryon  $N^*$  at the values of  $\kappa_l$  where we could identify a plateau. For the strange quark we take  $\kappa_s = 0.155$ , which produces a mass for the  $\phi$  meson of  $0.421(3)$  in lattice units. Using the mass of the nucleon in the chiral limit given in Table I, we find that the ratio of the mass of the  $\phi$  meson to the mass of the nucleon at the chiral limit is  $m_\phi/m_N = 1.002 \pm 0.025$ , which is very close to the physical ratio of  $1.087$  verifying that the value of  $\kappa_s = 0.155$  used is very close (within 10%) to the physical strange quark mass. We analyzed 202 configurations for the  $16^3 \times 32$  lattice [27] and 100 configurations for each of the  $24^3 \times 32$  and  $32^3 \times 64$  lattices.

#### A. The nucleon sector

In order to assess our methods of analysis, we first examine the results obtained for the nucleon using the standard interpolating field,

$$J_N(x) = \epsilon^{abc} (u_a^T(x) C\gamma_5 d_b(x)) u_c(x), \quad (14)$$

which can be local as given in Eq. (14) or constructed from smeared fields  $\tilde{u}$  and  $\tilde{d}$  instead of  $u$  and  $d$ . We denote the latter by  $\tilde{J}_N$ . In evaluating the nucleon correlator we can use  $J_N$  for the source and sink or use  $\tilde{J}_N^\dagger$  for the source and  $J_N$  for the sink. In general, denoting with  $H$  the appropriate hadronic state, the correlator  $C(t) = \int d^3x \langle 0 | J_H(x) J_H^\dagger(0) | 0 \rangle$  computed using local interpolating fields for the source and the sink is referred to as the local-local correlator, whereas the correlator  $\tilde{C}(t)$  computed using a local (smeared) field for the source and smeared (local) for the sink is referred to as local-smeared correlator. Finally the correlator,  $\hat{C}(t)$ , computed using smeared fields for both the source and the sink, is referred to as smeared-smeared correlator. In Fig. 1 we show results for the nucleon effective mass defined by

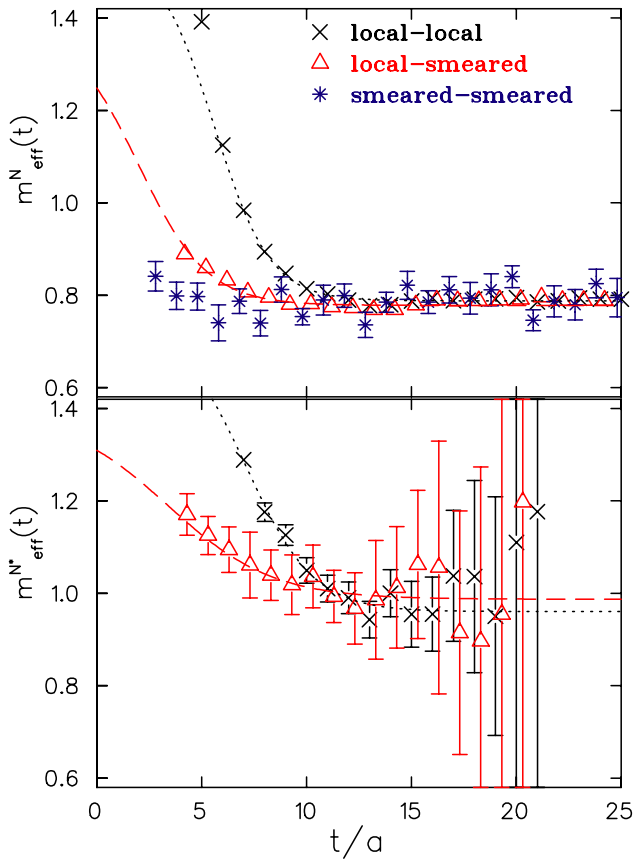


FIG. 1 (color online). The upper graph shows the effective mass for the nucleon (positive parity) and the lower graph for the  $N^*$  (negative parity) at  $\kappa_l = 0.153$ . The crosses show the results using the local-local correlator,  $C(t)$ , and Dirichlet b.c. and the open triangles using the local-smearred correlator,  $\tilde{C}(t)$  and antiperiodic b.c. shifted to the right for clarity. In the case of the nucleon, we also show results obtained using the smearred-smearred correlator  $\hat{C}(t)$  (asterisks) shifted to the left for clarity. The dotted and dashed lines are fits to the effective masses obtained using  $C(t)$  and  $\tilde{C}(t)$ , respectively, assuming two state dominance.

$$m_{\text{eff}}(t) = -\log \frac{C(t)}{C(t-1)} \quad (15)$$

on the lattice of size  $32^3 \times 64$  with Dirichlet boundary conditions. On the same figure we also show results obtained from  $\tilde{C}(t)$  with antiperiodic boundary conditions in the time direction. As can be seen, smearing improves the overlap with the nucleon ground state resulting in an earlier plateau. All the errors shown on our figures and given in the tables are statistical and they are determined using a jack-knife analysis.

We fit the effective mass assuming two state dominance to the form

$$m_{\text{eff}}(t) = m_0 - \log \frac{1 + ze^{-\Delta mt}}{1 + ze^{-\Delta m(t-1)}}, \quad (16)$$

where  $m_0$  is the mass of the ground state,  $\Delta m = m_1 - m_0$  is the mass gap between the ground state and the first excited state, and  $z$  is the ratio of the overlap of the interpolating field with the first excited state as compared to the ground state. For the nucleon sector  $m_0$  gives the mass of the nucleon and  $\Delta m$  the mass gap between the nucleon and the  $N(1440)$  state. The values of  $m_0$  and  $\Delta m$  determined from fitting the effective mass derived either from  $C(t)$  or  $\tilde{C}(t)$  are in agreement. The errors on the mass gap  $\Delta m$  however are large not allowing an accurate determination of the mass of the excited state. The fact that the ground state overlap is enhanced, as compared to that of the first excited state when smearing is used, is confirmed by the decrease in the value of  $z$  by a factor of about 20. Smearing both source and sink tends to suppress even further the excited state contributions and decorrelates the results at successive time slices. The mass extracted by fitting the smearred-smearred correlator,  $\hat{C}(t)$ , to a single exponential is  $m_N = 0.789(9)$  consistent with that extracted from the local-smearred correlator. However, as can be seen in Fig. 1, the statistical error on the smearred-smearred results at each time slice is larger as compared to the errors of the local-smearred results due to the gauge noise introduced at the sink. Such errors will make it difficult to distinguish two closely lying states, and therefore in the case of the pentaquark system we will mostly use local-local and local-smearred correlators.

An important test that distinguishes particle states from scattering states is the scaling of the spectral weights of local correlators with the spatial volume of the lattice [17,22]. Expanding the correlator computed on a lattice of spatial size  $L$  in terms of states with the same quantum numbers as the interpolating field, one obtains

$$C_L(t) = \sum_{\alpha} W_L^{\alpha} e^{-E_L^{\alpha} t}. \quad (17)$$

For a single particle state the weights  $W_L^{\alpha}$  are of order one whereas for a scattering state consisting of two weakly interacting particles well below the resonance are of order  $1/L^3$ . Furthermore, for a single particle state,  $E_L^{\alpha}$  determines the mass of the state and should be volume independent for large enough volumes. For a scattering state that is not an s-wave, on the other hand,  $E_L^{\alpha}$  is volume dependent since it involves the relative momentum of the two particles, a fact which on the lattice means that each particle carries equal momentum in units of  $2\pi/L$ . In the case of the nucleon, we know that we have a single particle state and we can check how reliably we can extract these weights. In Fig. 2 we plot the ratio of the local-local correlator  $C_{16}(t)$  to  $C_{24}(t)$  (computed on the lattices of size  $16^3$  and  $24^3$ , respectively) for the nucleon and the  $N^*$ . In a time interval where a single state dominates (plateau region), assuming its mass is volume independent, the ratio of correlators is equal to the ratio of weights  $W_{16}/W_{24}$ . This ratio should be one for a single particle

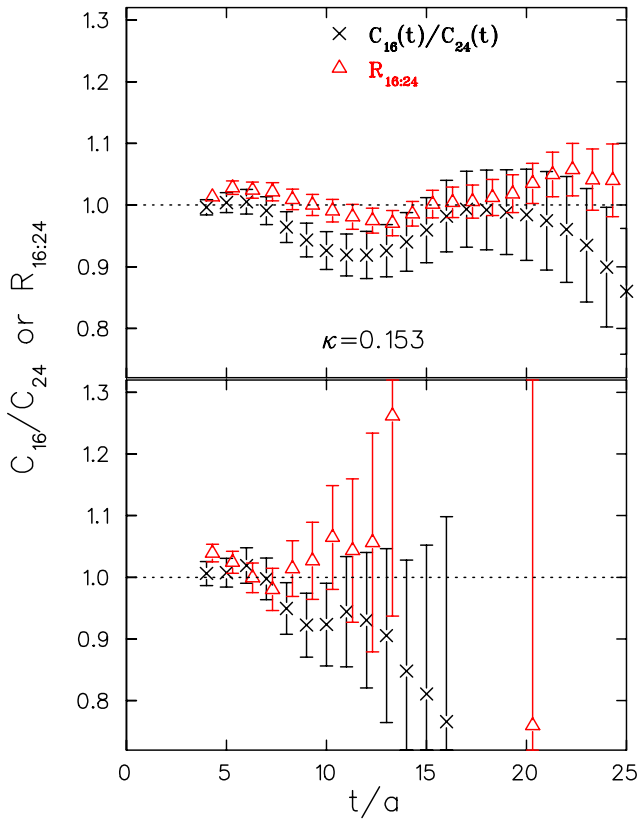


FIG. 2 (color online). We show the ratio  $C_{16}(t)/C_{24}(t)$  (crosses) and the ratio  $R_{16:24}^H$  (open triangles with a small shift to the right for clarity) as a function of the time separation in lattice units. The upper graph shows results for the nucleon and the lower for  $N^*$  at  $\kappa_l = 0.153$ .

state. As can be seen, the ratio of correlators is approximately one. In the same figure we also show the ratio

$$R_{L_1:L_2}^H \equiv \frac{C_{L_1}(t)e^{m_{\text{eff},L_1}(t)}}{C_{L_2}(t)e^{m_{\text{eff},L_2}(t)}}, \quad (18)$$

where with  $H$  we denote the nucleon or the  $N^*$  and we have taken  $L_1 = 16$  and  $L_2 = 24$ . This ratio corrects small finite size effects on the mass and in the plateau region is again equal to  $W_{L_1}/W_{L_2}$ . As can be seen,  $R_{L_1:L_2}^H$  indeed improves the signal, in particular, for the nucleon, giving better agreement with unity, which is the expected result.

## B. The two-pion sector

Having tested our techniques for a single particle state, we now verify that they can be applied for two-particle scattering states. For this test we choose the two-pion system in the isospin two channel where no low lying resonances are expected. We consider five interpolating fields:

$$\begin{aligned} J_1^{2\pi}(x) &= J_1^\pi(x)J_1^\pi(x), & J_1^\pi(x) &= \bar{d}(x)\gamma_5 u(x), \\ J_2^{2\pi}(x) &= J_2^\pi(x)J_2^\pi(x), & J_2^\pi &= \bar{d}(x)\gamma_5\gamma_0 u(x), \\ J_3^{2\pi}(x) &= J_3^\pi(x)J_3^\pi(x), & J_3^\pi &= \bar{d}(x)\gamma_5\hat{e}_\mu\gamma_\mu u(x), \\ J_4^{2\pi}(x) &= J_0^\rho(x)J_0^\rho(x), & J_0^\rho &= \bar{d}(x)\gamma_0\sum_{i=1}^3\gamma_i u(x), \\ J_5^{2\pi}(x) &= \sum_{i=1}^3 J_i^\rho(x)J_i^\rho(x), & J_i^\rho(x) &= \bar{d}(x)\gamma_i u(x). \end{aligned} \quad (19)$$

The first three are products of pion interpolating fields whereas the last two are products of rho-type interpolating fields. As we already pointed out, the energy of a scattering state of two hadrons  $h_1$  and  $h_2$  depends on the spatial size  $L$  of the lattice and is given by

$$E_{h_1 h_2}^n = \sqrt{m_{h_1}^2 + n\left(\frac{2\pi}{L}\right)^2} + \sqrt{m_{h_2}^2 + n\left(\frac{2\pi}{L}\right)^2}, \quad (20)$$

$$n = 0, 1, \dots$$

where we have suppressed the  $L$  index on the energy. In Fig. 3 we show the effective mass for a single pion using the interpolating fields  $J_1^\pi(x)$ ,  $J_2^\pi(x)$ , and  $J_3^\pi(x)$  for our three lattices. As expected  $J_1^\pi(x)$ , routinely used in lattice calculations, and its variant  $J_2^\pi(x)$  have the largest overlap with the pion. All three yield consistent results for the pion mass. For the two-pion system the interpolating field  $J_3^{2\pi}(x)$  is very noisy as compared to the other four and we do not include it in the figure. We obtain the best overlap with the two-pion ground state when using  $J_1^{2\pi}(x)$  with  $J_2^{2\pi}(x)$  and  $J_5^{2\pi}(x)$  being the next best. Again all interpolating fields produce consistent two-pion energies for large enough time separation. For lattices  $16^3 \times 32$  and  $32^3 \times 64$ , the time extent is sufficient to have a large plateau region after suppression of excited state contributions. For the  $24^3 \times 32$  lattice this occurs for time separations  $t/a > 22$  limiting the fit range to a few time slices.

We perform a variational analysis using the interpolating fields defined in Eq. (19) excluding  $J_3^{2\pi}$ , which means that in Eq. (9) we take  $M = 4$ . To check we also compute the eigenvalues by the second method of analysis, namely, by projecting using Eq. (11) to an  $N \times N$  matrix where we take  $N = 3$ . We find two distinct eigenstates for which we also construct the best interpolating field using the eigenvectors  $\mathcal{V}_n$ . For this system, had we used only interpolating fields  $J_1$  and  $J_4$  the resulting eigenvalues would be consistent with the ones obtained within the larger variational set. This is an important observation since it demonstrates that using two interpolating fields which have very good overlap with two low lying states we can accurately determine them by diagonalizing the  $2 \times 2$  correlation matrix. The effective mass determined for the two

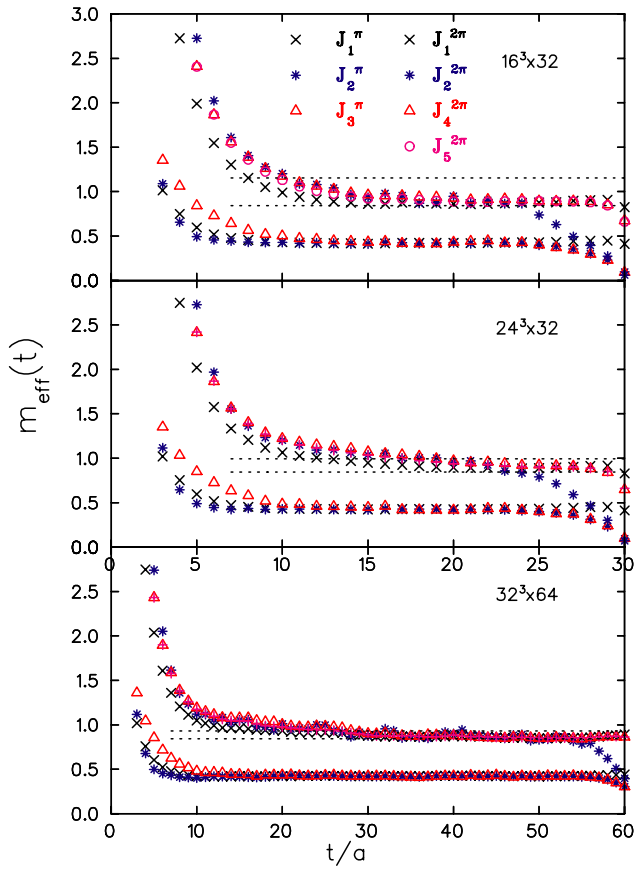


FIG. 3 (color online). The effective mass at  $\kappa_l = 0.153$  as a function of  $t/a$  for the lattice of size  $16^3 \times 32$  (top),  $24^3 \times 32$  (middle), and  $32^3 \times 64$  (bottom). The set of results with the lower value are obtained using one pion interpolating fields,  $J_1^\pi$  (crosses),  $J_2^\pi$  (asterisks), and  $J_3^\pi$  (open triangles). The set with the higher value corresponds to the two-pion interpolating fields,  $J_1^{2\pi}$  (crosses),  $J_2^{2\pi}$  (asterisks),  $J_4^{2\pi}$  (open triangles), and  $J_5^{2\pi}$  (circles). The dotted lines are the two lowest two-pion scattering states  $E_{2\pi}^0$  and  $E_{2\pi}^1$ .

eigenvalues  $\Lambda_n$  is shown in Fig. 4 for our three lattices. In all cases the effective mass extracted from the lowest energy eigenvalue (largest  $\Lambda$ ) is in agreement with that extracted from the correlator that uses the interpolating field  $J_1^{2\pi}$ . As the spatial extension of the lattice increases, a larger time separation is needed for the effective mass to reach the energy of the s-wave scattering state  $E_{2\pi}^0$ . Since in this system the low lying states are two-particle scattering states, this clearly demonstrates that the two lowest eigenvalues do not correspond to a given value of the relative momentum carried by each particle but they are an admixture of states having nonzero relative momentum that mix with the state with zero relative momentum. The energy difference,  $E^n - E^{n-1}$ , between different relative momentum states decreases like  $1/L^2$  and therefore a larger time interval is needed in order to reach the ground state as  $L$  increases. This can be seen in Fig. 4 where for the  $16^3$  lattice the plateau for the ground state is reached for

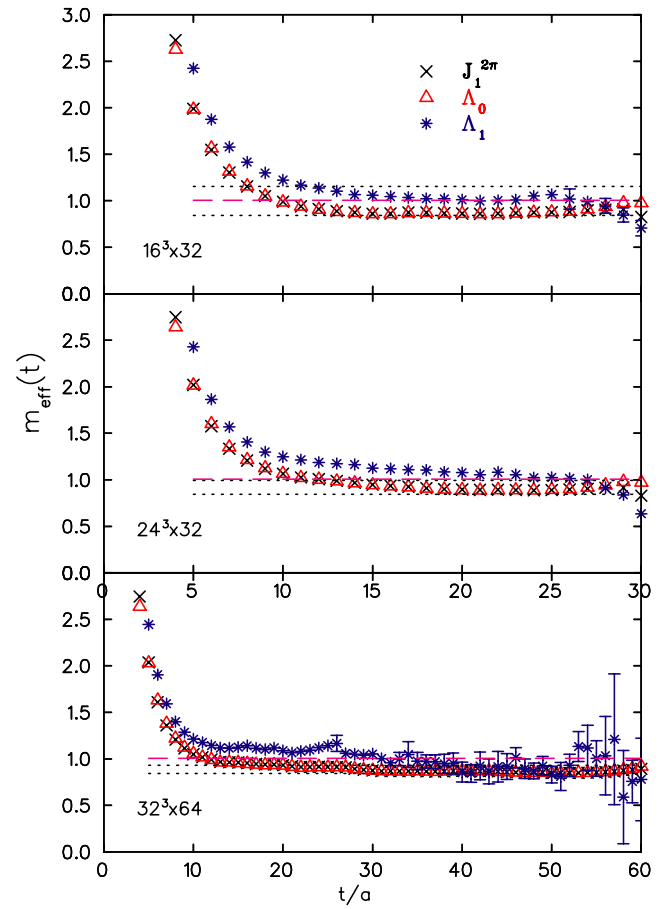


FIG. 4 (color online). The effective mass at  $\kappa_l = 0.153$  extracted from the correlator using the interpolating field  $J_1^{2\pi}$  (crosses) and from the two largest eigenvalues  $\Lambda_0$  (open triangles) and  $\Lambda_1$  (asterisks) for the lattice of size  $16^3 \times 32$  (upper graph),  $24^3 \times 32$  (middle graph), and  $32^3 \times 64$  (lower graph). The dotted lines are the two lowest energy two-pion scattering states  $E_{2\pi}^0$  and  $E_{2\pi}^1$ . The dashed line is the lowest energy two-rho scattering state  $E_{2\rho}^0$ .

$t/a > 13$  whereas for the  $24^3$  we need  $t/a > 23$  and for the  $32^3$   $t/a > 30$ . These values determine the smallest value of the lower time range to be used in fitting the effective masses to a constant. If one would like to reduce the lower fit range then fitting to a two-exponential form using Eq. (16) is essential. A similar behavior is also observed for the second eigenstate: On the  $16^3$  the two-rho scattering state  $E_{2\rho}^0$  is the second lowest energy state since  $E_{2\pi}^1$  is higher and a clear plateau is seen for  $t/a > 17$ . Going to the larger  $24^3$  lattice  $E_{2\pi}^1$  decreases becoming about equal to  $E_{2\rho}^0$  with a plateau that sets in for  $t/a \sim 25$  resulting in a fit range limited to three points. This explains why the energy extracted is higher on this lattice than  $2m_\rho$  as can be seen in Fig. 5, where we plot the mass extracted from fitting the effective mass in the available plateau region versus the spatial lattice size. Finally, despite the fact that on the  $32^3$  lattice  $E_{2\pi}^1 < E_{2\rho}^0$  the two-rho state dominates the time

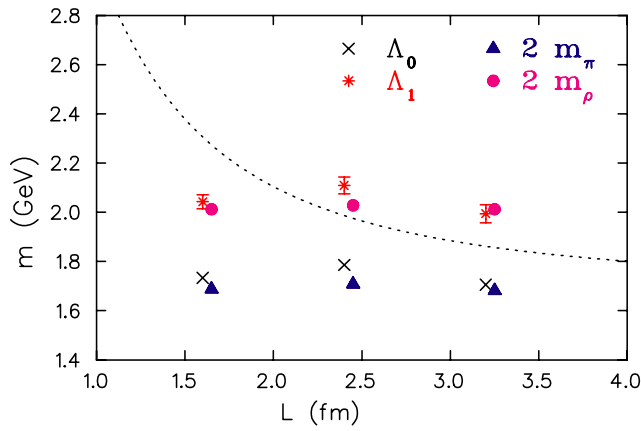


FIG. 5 (color online). The mass at  $\kappa_l = 0.153$  extracted from fitting the plateau of the effective mass of the lowest energy eigenvalue (filled triangles) and the second higher energy eigenvalue (filled circles shifted to right for clarity) as a function of the spatial length of the lattice  $L$ . Also shown are results for twice the mass extracted from the pion correlator (crosses) and rho correlator (asterisks). The dotted line is the two-pion scattering energy  $E_{2\pi}^1$ .

dependence of the second eigenvalue for  $30 \leq t/a \leq 40$ . For  $t/a > 40$  the effective mass becomes consistent with  $E_{2\pi}^1$  but in this time range the statistical errors become too large to clearly distinguish the  $E_{2\pi}^1$  scattering state. Therefore fitting the effective mass in a time range 30–40 or extending the upper fit range affects very little the resulting value thereby obtaining the rather accurate measurement of  $E_{2\rho}^0$  displayed in Fig. 5. Note that corrections due to interactions between the two pions cannot be seen on the scale of this figure assuming that we can use the physical scattering length in Luscher's result [28]. It must be noted that on the large lattice fitting in the plateau-like region in the time range  $15 < t/a < 30$  would yield an incorrect higher value for the energy. Therefore this demonstrates that for lattices of spatial extent of about 3 fm we need a time separation of at least  $40a$  to obtain correctly the energy of the two-rho state making the use of Dirichlet b.c. essential. To verify that the reason the plateau region starts at relative large time separations is due to contamination of states with higher relative momentum, we perform on the small lattice an explicit momentum projection to two particles each carrying zero momentum. This is done by evaluating the correlation matrix

$$C_{j's'k's}(t) = \sum_{\mathbf{x}, \mathbf{y}} \langle 0 | J_j^{s'}(\mathbf{x}, t) J_{j'}^{s'}(\mathbf{y}, t) J_k^{s\dagger}(0) J_k^{s\dagger}(0) | 0 \rangle, \quad (21)$$

where  $s, s'$  denotes the pion or the rho.

In Fig. 6 we compare the eigenvalues obtained when we carry out the zero momentum projection for each particle to our previous (unprojected) results. As can be seen for both eigenstates, the plateau region starts at earlier time

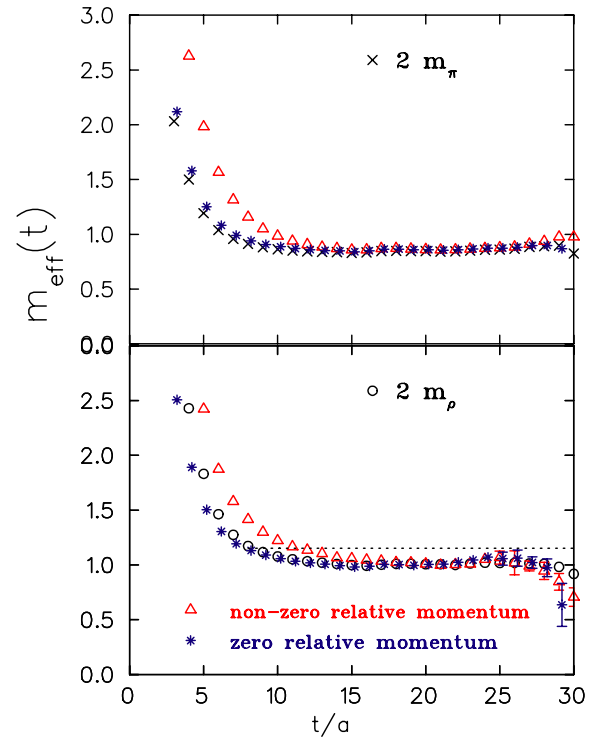


FIG. 6 (color online). The upper graph shows the effective mass for the lowest energy eigenstates and the lower graph the effective mass for the second higher energy eigenstate. In both graphs we show data with projection to zero relative momentum using Eq. (21) (asterisks shifted to the right for clarity) and without explicit projection (open triangles) for the lattice of size  $16^3 \times 32$  at  $\kappa_l = 0.153$ . We also show twice the effective mass extracted from a single pion (crosses in upper graph) and rho correlator (circles in lower graph). The dotted line is the two-pion scattering state  $E_{2\pi}^1$ .

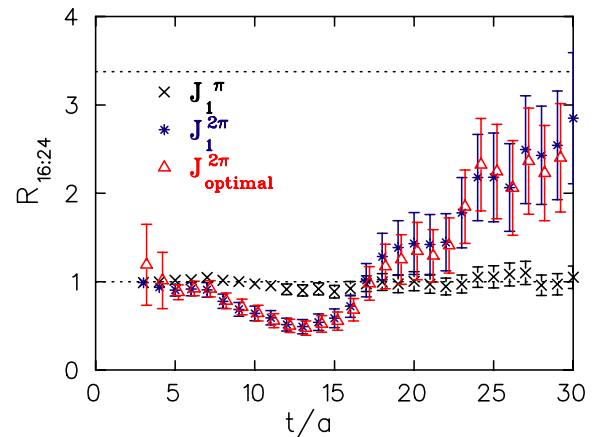


FIG. 7 (color online). The ratio  $R_{16:24}$  at  $\kappa_l = 0.153$  for one and two-pion states using interpolating field  $J_1^\pi(x)$  (crosses) and  $J_1^{2\pi}(x)$  (asterisks) as a function of  $t/a$ . The ratio  $R_{16:24}$  extracted from correlators using the optimal combination  $J_{\text{optimal}}(x)$  for the lowest eigenstate of the two-pion system is shown by the open triangles shifted to the right for clarity. The dotted lines show the expected value of the ratio for a single particle state and a two-particle scattering state.

separations. In fact for  $t/a > 6$  the projected two-particle correlator is the same as the product of the single particle correlators. For large enough time separations, the unprojected eigenvalues approach the correct values  $E_{2\pi}^0$  and  $E_{2\rho}^0$  giving an energy gap  $E_{2\rho}^0 - E_{2\pi}^0 \sim 320$  MeV at  $\kappa_l = 0.153$ . The mass gap between the  $\Theta^+$  and the KN s-wave scattering state is not known at this value of  $\kappa_l$ . However, as we will discuss when presenting the chiral extrapolation of our results, the mass gap between our candidate pentaquark resonance and  $E_{KN}^0$  increases with the quark mass to about 170 MeV at  $\kappa_l = 0.153$  in the negative parity channel. This estimated smaller gap can make the study of the pentaquark system harder.

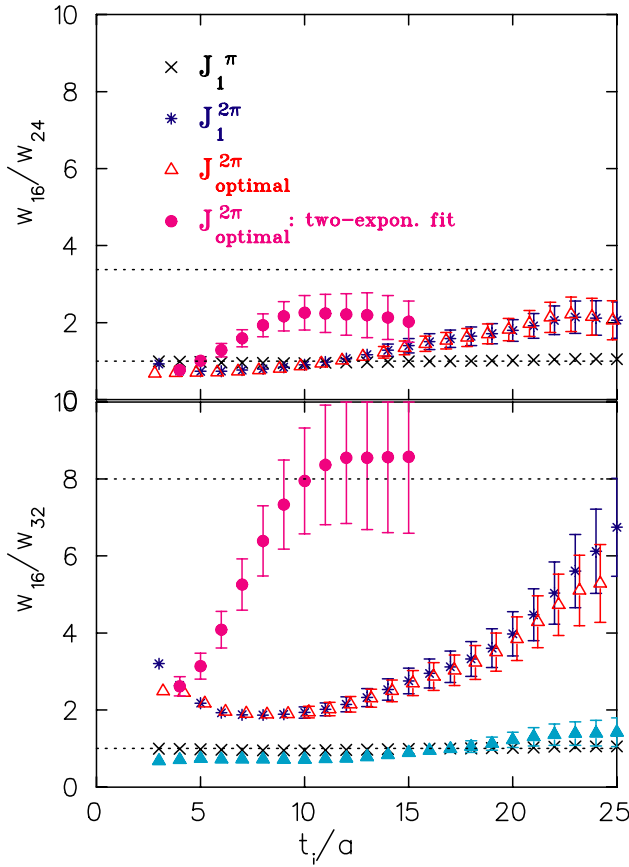


FIG. 8 (color online). The ratio of spectral weights  $w_{16}/w_{24}$  (upper graph) and  $w_{16}/w_{32}$  (lower graph) as a function of the lower fit range  $t_i/a$  at  $\kappa_l = 0.153$ . Asterisks denote results extracted from the correlator with  $J_1^{2\pi}(x)$ , open triangles and filled circles from the correlator with  $J_{\text{optimal}}(x)$  fitted to a single exponential and to a sum of two exponentials, respectively. For comparison we also show these ratios for the single pion state using  $J_1^\pi(x)$  (crosses). The upper fit range is fixed to 26 for the  $16^3 \times 32$  lattice and to 56 for the  $32^3 \times 64$  lattice. On the lower graph with the filled triangles we show results for the ratio of spectral weights  $w_{16}/w_{32}$  when the upper fit range for the large lattice is fixed to 26. The dotted lines show the expected value of the ratios for a single particle state and a two-particle scattering state.

Having identified the two lowest eigenstates within our variational basis, we study the spectral weights of these states. In Fig. 7 we show the ratio  $R_{16:24}$  for the pion when using the interpolating field  $J_1^\pi(x)$  and for two pions when using  $J_1^{2\pi}(x)$  as well as  $J_{\text{optimal}}$ . This ratio is unity for the pion as expected, whereas for the two-pion system it increases approaching the expected ratio of 3.4 for  $t_i/a > 25$  when the s-wave two-pion scattering state dominates. For the lattice of spatial extent 32 this happens for  $t/a > 30$  and therefore  $R_{16:32}$  stays close to unity up to about  $t/a = 30$  which is the largest time separation for which it can be constructed. Instead of  $R_{16:32}$  we can extract the spectral weights by fitting the correlator to a single exponential or to a sum of two exponentials. This allows one to take into account information from the full time extent of the lattice. We fix the upper fit range to 26 in lattice units for the lattices of temporal extent  $N_t = 32$  and to 56 for the lattice with  $N_t = 64$ . We show in Fig. 8 the ratio of spectral weights  $w_{16}/w_{24}$  and  $w_{16}/w_{32}$  for the lowest state. What can be seen is that both ratios extracted using a single exponential fit increase approaching the expected value for a scattering state. Fitting to a sum of two exponentials, we obtain ratios that approach the expected value at much smaller time separations albeit with larger errors. However, if instead of 56 we take an upper fit range of 26 for the large lattice either using single or double exponential fits, the ratio  $w_{16}/w_{32}$  stays close to unity leading to the wrong conclusion. We show the corresponding ratios for the second eigenstate in Fig. 9 using a single exponential.

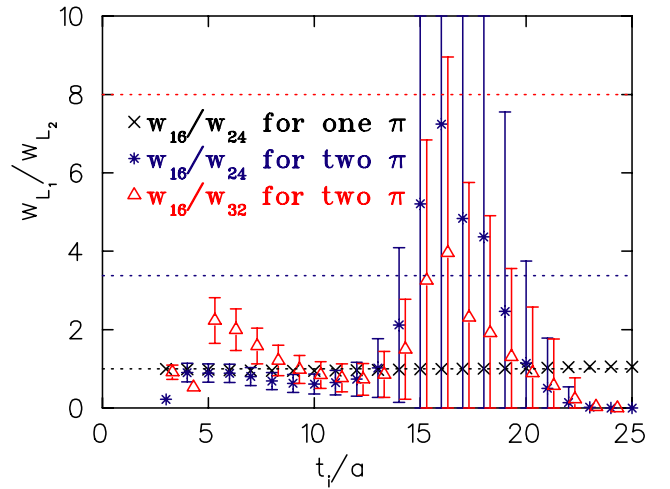


FIG. 9 (color online). The ratio of spectral weights  $w_{16}/w_{24}$  extracted from the correlators with interpolating field  $J_{\text{optimal}}(x)$  (asterisks) for the first excited state of the lower fit range  $t_i/a$ . The corresponding ratio  $w_{16}/w_{32}$  is shown with the open triangles. The dotted lines show the expected value of the ratio for a single particle state and a two-particle scattering state. The crosses show for comparison the ratio of spectral weights for one pion state extracted from the correlator using interpolating field  $J_1^\pi(x)$ .

Even though the errors on the correlators are small the error on the ratio of spectral weights is too large to lead to a definite conclusion. Had we used a sum of two exponentials, the errors would be even larger.

### C. The pentaquark sector

The first experimental indication for the existence of a pentaquark state came when the LEPS collaboration [1] detected a resonance with mass  $1540 \pm 10$  MeV and width less than 25 MeV in accord with the predictions of the chiral soliton model [6]. This small width is surprising since, lying about 100 MeV above the KN threshold, it is expected to readily decay to KN. Since the observation of the first signal for  $\Theta^+$  was reported, several other experiments were carried out, some confirming its existence [3] and others not [4,5].

Whether lattice QCD supports the existence of a pentaquark state is also unclear [20]. The study of resonances in lattice QCD is in its infancy and therefore it comes with no surprise that identifying the  $\Theta^+$  on the lattice turned out to

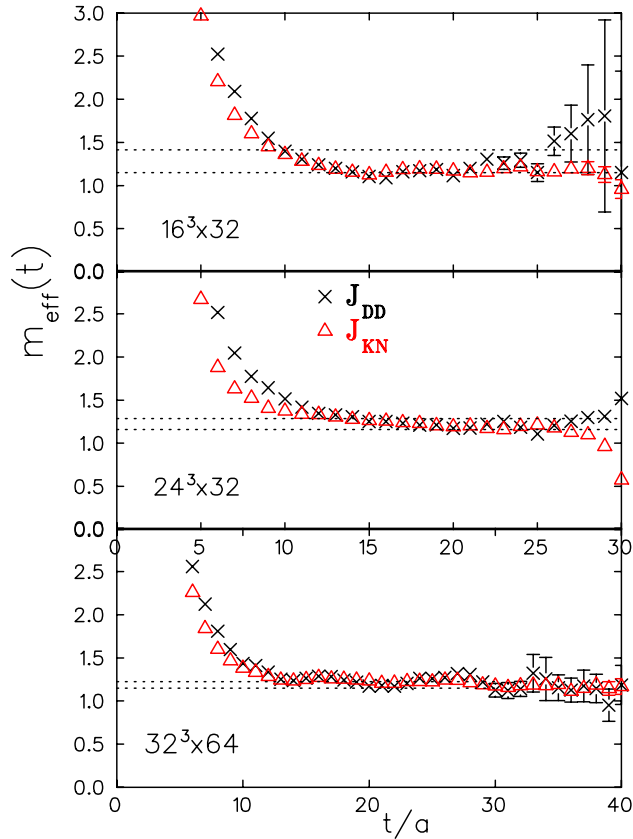


FIG. 10 (color online). The effective mass for the pentaquark in the negative parity channel for lattices of size  $16^3 \times 32$  (upper graph),  $24^3 \times 32$  (middle graph), and  $32^3 \times 64$  (lower graph) at  $\kappa_l = 0.153$ . The crosses show the results obtained from correlators using  $J_{DD}$  and the open triangles using  $J_{KN}$ . The dotted lines show  $m_N + m_K$  and  $E_{KN}^1$ .

be a difficult task. In the two-pion system, scaling of the spectral weights  $W$  with the spatial volume was observed for large time separations. We will use the largest available time separations in applying the same analysis in the pentaquark system. Clearly, whether this criterion can be used in practice will depend on the size of the statistical errors.

In Figs. 10 and 11, we show the effective mass for both the negative and positive parity states evaluated on our three lattices at  $\kappa_l = 0.153$  for isospin zero using the local interpolating fields  $J_{DD}$  and  $J_{KN}$ . What can be seen from these figures is that both interpolating fields yield consistent plateaus in both channels with the KN-interpolating field yielding smaller errors in the negative parity channel than the diquark-diquark interpolating field, whereas in the positive parity channel the opposite is true. We also see that the errors even at this heavy pion mass are large especially for the positive parity channel limiting the determination of the large time behavior. This means that extracting the spectral weights for the positive parity channel accurately enough for large time separations to test scaling will not be possible. Therefore for the positive parity channel we can

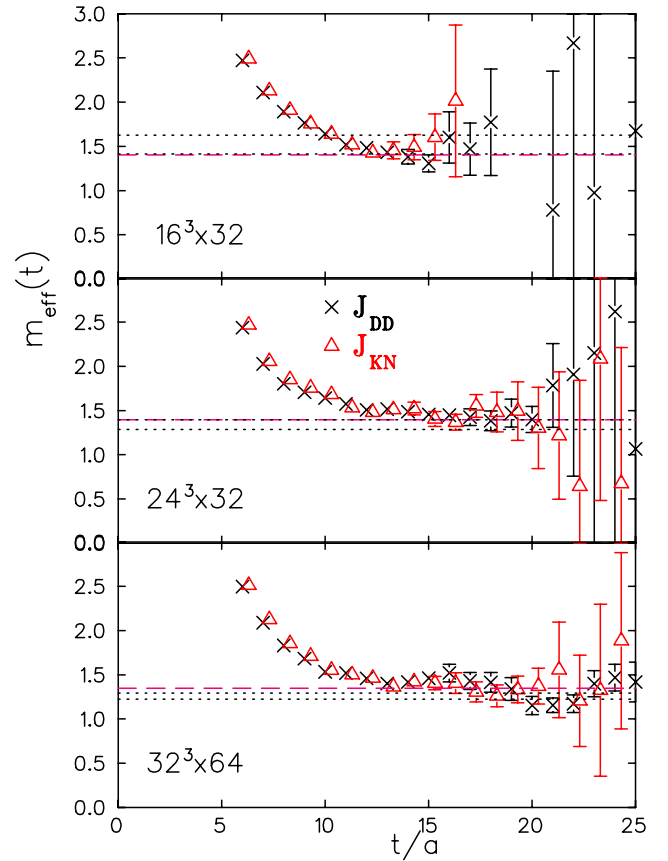


FIG. 11 (color online). The effective mass for the pentaquark in the positive parity channel at  $\kappa_l = 0.153$ . The dotted lines show  $E_{KN}^1$  and  $E_{KN}^2$  and the dashed line  $m_K + m_{N^*}$ . The rest of the notation is the same as that of Fig. 10.

only look for volume dependence in the extracted energy of the states. This energy can be determined either by fitting the effective mass in the plateau range to a constant or, allowing for two states, to the form given in Eq. (16). The latter is especially important when using local-local correlators, since excited states have large contributions up to time separation of about  $14a$ . Our aim is to detect a resonance, which is higher than the scattering KN state and therefore it is crucial to be able to fit in a time range where it is still the dominant state. This is expected to hold for time intervals less than about  $t/a \sim 20$  or  $t \lesssim 10 \text{ GeV}^{-1}$ . The values obtained for the mass, fitting within this range using either  $J_{DD}$  or  $J_{KN}$ , are given in Table II for all three lattices. From these values, we can conclude that, either using the diquark-diquark or the KN local interpolating field, the masses that we find are within each other's error. In the positive parity channel the systematic volume effect of a decrease in the mass with the increase of the lattice size, characteristic of a scattering state, is not observed.

The standard approach to suppress excited state contributions improving the effective mass plateaus is to use smearing. We use Wuppertal smeared interpolating fields on the large lattice imposing antiperiodic boundary con-

ditions in the temporal direction. As can be seen in Fig. 12, where we show results for  $\kappa_l = 0.153$ , smearing the source but keeping the sink local suppresses excited state contributions. Note that, within our statistical errors, the effective mass with smeared source on half the lattice is in agreement with the results from the local correlator at larger times leading to the same plateau values. This justifies the use of antiperiodic b.c. As we already pointed out, if the sink is also smeared the gauge noise increases making identification of two close-by states impossible. Therefore for the rest of the results we will apply smearing only at the source.

Having confirmed that both local and smeared interpolating fields as well as the KN and diquark-diquark interpolating fields lead to consistent values for the mass, we perform the variational analysis described in Sect. II. As in the two-pion system, the eigenvalues will still be contaminated by scattering states with nonzero relative momentum. This is particularly severe on the large lattice where the scattering KN states are very close in energy as can be seen in Figs. 10 and 11. If within our variational basis we have interpolating fields that have good overlap with the pentaquark resonance then the two energy eigenvalues

TABLE II. The first column gives the interpolating field, the second column gives the mass of the pentaquark extracted by fitting the effective mass to a constant in the plateau region, and the third column gives the mass extracted by fitting to the form given in Eq. (16) for the lattice of size  $16^3 \times 32$ . The corresponding quantities for the other two lattices are given in the next four columns. We give results at values of  $\kappa_l = 0.153$  and  $0.155$  for both parity states. The  $\chi^2/\text{d.o.f}$  for these fits is less than one.

	$16^3 \times 32$		$24^3 \times 32$		$32^3 \times 64$	
$\kappa_l = 0.153$						
Negative parity						
Operator	<i>am</i> (1 exp)	<i>am</i> (2 exp)	<i>am</i> (1 exp)	<i>am</i> (2 exp)	<i>am</i> (1 exp)	<i>am</i> (2 exp)
$J_{DD}$	1.172(14)	1.174(14)	1.236(14)	1.240(15)	1.237(12)	1.234(13)
$J_{KN}$	1.173(9)	1.180(9)	1.232(15)	1.239(17)	1.239(9)	1.236(9)
$J_{\text{optimal}}$	1.178(14)	1.176(16)	1.232(14)	1.253(23)	1.235(9)	1.230(9)
Positive parity						
$J_{DD}$	1.432(50)	1.376(59)	1.485(30)	1.449(48)	1.382(30)	1.423(25)
$J_{KN}$	1.488(51)	1.411(87)	1.479(44)	1.434(64)	1.400(36)	1.414(35)
$J_{\text{optimal}}$	1.502(135)	...	1.448(52)	1.465(167)	1.462(46)	1.444(68)
$\kappa_l = 0.155$						
Negative parity						
Operator	<i>am</i> (1 exp)	<i>am</i> (2 exp)	<i>am</i> (1 exp)	<i>am</i> (2 exp)	<i>am</i> (1 exp)	<i>am</i> (2 exp)
$J_{DD}$	0.977(44)	0.938(23)	1.014(19)	1.013(23)	1.031(15)	1.034(15)
$J_{KN}$	0.947(15)	0.937(17)	0.998(20)	1.002(26)	1.023(10)	1.020(11)
$J_{\text{optimal}}$	0.952(19)	0.929(27)	1.006(15)	1.012(32)	1.022(13)	1.020(14)
Positive parity						
$J_{DD}$	1.300(67)	1.184(92)	1.323(33)	1.316(44)	1.308(26)	1.250(49)
$J_{KN}$	1.374(60)	1.283(129)	1.274(48)	1.255(67)	1.230(42)	1.218(47)
$J_{\text{optimal}}$	1.457(89)	...	1.256(57)	1.283(179)	1.290(75)	1.259(116)

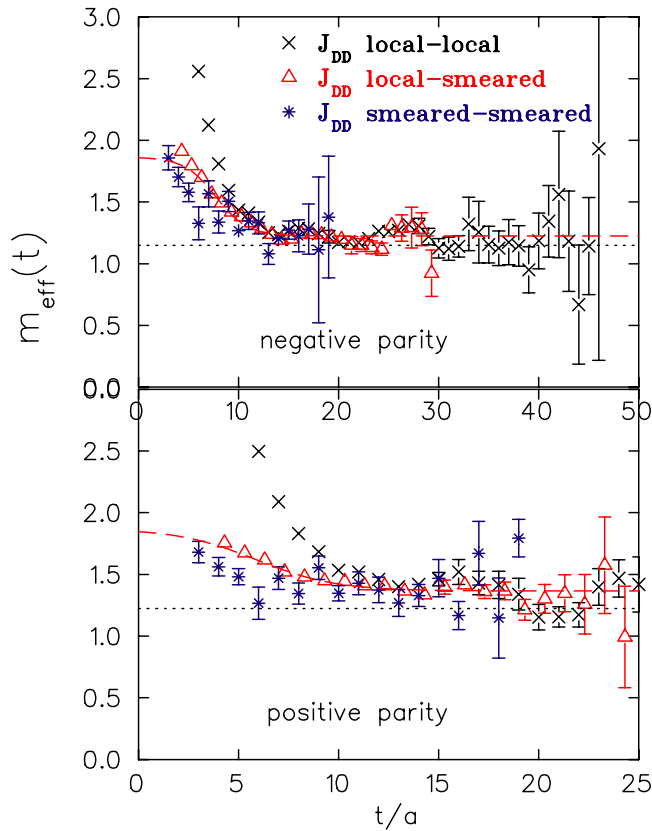


FIG. 12 (color online). The upper graph shows the pentaquark effective mass for the negative parity channel and the lower graph for the positive parity channel at  $\kappa_l = 0.153$  on the lattice of size  $32^3 \times 64$ . The crosses show results obtained from the local-local correlator  $C(t)$ , the open triangles results from the local-smearred correlator  $\tilde{C}(t)$  shifted to the right, and the asterisks results from the smearred-smearred correlator  $\tilde{C}(t)$ . The diquark-diquark interpolating field is used in all correlators. The dashed line is a two-exponential fit to the local-smearred results. The dotted line shows  $E_{KN}^0$  for the negative and  $E_{KN}^1$  for the positive parity channel.

should yield the KN scattering states and the  $\Theta^+$ . The choice of the diquark-diquark interpolating field is based on the expectation that it should approximate well the structure of  $\Theta^+$ . However, if this is not the case then we will not be able to obtain the resonance state as the second eigenvalue of the  $2 \times 2$  correlation matrix. The lowest eigenstate will be accurately determined and, allowing for large enough time separations, it should produce the s-wave KN scattering state in the negative channel and the p-wave KN scattering state in the positive channel. If there is an admixture of a resonance state, then we expect the spectral weights to show a different behavior from that observed in the two-pion system where the only low lying states are scattering states. In the positive parity channel only KN scattering states with nonzero relative momentum contribute. Therefore the lowest energy is expected to decrease as the spatial volume of the lattice increases according to Eq. (20). Since we expect the errors on the

spectral weights to be too large in this channel to allow us to test scaling, the only option is to study the volume dependence of the energy on the spatial length of the lattice. However, in the positive parity channel the s-wave  $KN^*$  scattering state is allowed. The energy of this state is shown in Fig. 11. On the small lattice the value of the smallest relative momentum  $2\pi/L$  is such that, at  $\kappa_l = 0.153$  using the masses given in Table I,  $E_{KN^*}^0$  comes out very close to  $E_{KN}^1$  whereas for the two larger lattices is higher. Therefore if the two lowest eigenstates are the  $KN^*$  and KN scattering states, then we expect the energy gap  $|E_{KN}^1 - E_{KN^*}^0|$  while being almost zero on the small lattice to increase for the other two. Clearly the existence of the  $KN^*$  scattering state complicates the identification of a pentaquark resonance also in the positive parity channel and would require at least a  $3 \times 3$  or even a  $4 \times 4$  correlation matrix to allow us to resolve three different states. A very accurate determination of the spectral weights for the three lowest states will be needed in order to distinguish the KN and  $KN^*$  scattering states from a resonance. This is beyond the scope of this work. Our working hypothesis is that if the  $\Theta^+$  is present then it should dominate the correlator in the appropriate time range and to have the largest coupling to the KN scattering state.

In Fig. 13 we show effective masses determined from the two eigenvalues  $\Lambda_0(t)$  and  $\Lambda_1(t)$  of the correlation matrix  $C(t)_{DD;KN}$  at  $\kappa_l = 0.155$ . The behavior at  $\kappa_l = 0.153$  discussed up to now is similar. We observe that, like in the case of the two-pion system, the effective mass derived from the lowest energy eigenvalue is consistent with that obtained from either interpolating field  $J_{DD}$  or  $J_{KN}$ . On the same figure we also show the effective mass obtained from the eigenvalues  $\tilde{\Lambda}_0(t)$  and  $\tilde{\Lambda}_1(t)$  of the correlation matrix  $\tilde{C}(t)_{DD;KN}$ , which involves local-smearred correlators of the two interpolating fields  $J_{DD}$  and  $J_{KN}$  and antiperiodic boundary conditions in the temporal direction. Again both local-local and local-smearred results yield the same plateaus with smearing suppressing excited state contributions. The main observation is that the first excited state behaves differently in the positive and negative parity channels: The negative parity channel is very high in energy and poorly determined. This is puzzling since if the diquark-diquark operator has good overlap with the  $\Theta^+$  then we would have expected it to be the first excited state of this correlation matrix with the ground state being the KN scattering state. In fact, if we compare the overlap of  $J_{DD}$  with the ground state to that obtained with  $J_{KN}$ , we find that it is about 50 times smaller. This raises questions as to how well a local diquark description approximates the structure of a pentaquark resonance. In the positive parity channel we obtain two distinct eigenstates very close together. From our study of the two-pion system, we know that the eigenvalues, in general, will not have a definite relative momentum but will be contaminated with states with higher relative momenta and therefore it becomes a

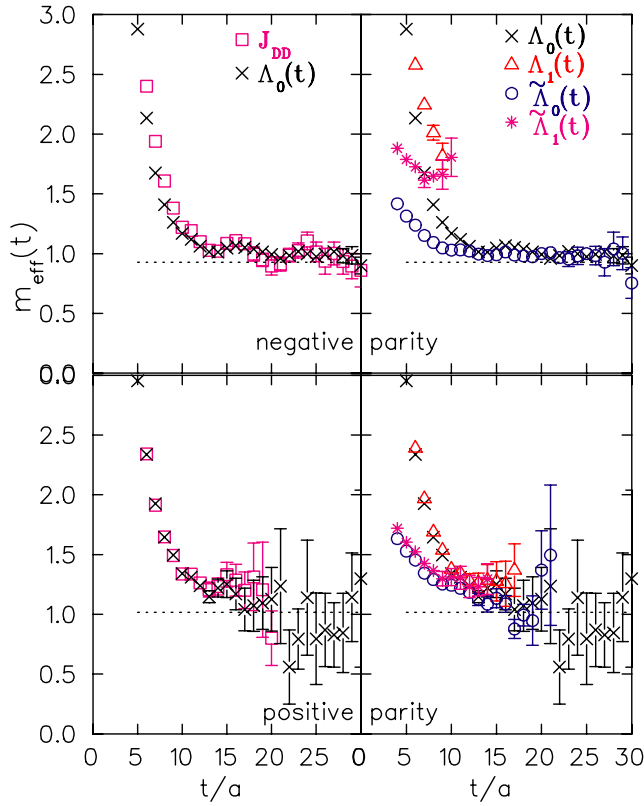


FIG. 13 (color online). The upper graphs show the effective mass for the negative parity and the lower graphs for the positive parity channels at  $\kappa_l = 0.155$  on the lattice of size  $32^3 \times 64$ . The squares on the left two graphs denote the results extracted from the correlators with the local interpolating field  $J_{DD}$ . The crosses on all four graphs show the effective mass, derived from the eigenvalue  $\Lambda_0(t)$  of  $C_{DD:KN}$ . On the graphs on the right, the open triangles denote results derived from  $\Lambda_1(t)$ , whereas the circles and asterisks are results extracted from the eigenvalue  $\tilde{\Lambda}_0(t)$  and  $\tilde{\Lambda}_1(t)$  from the diagonalization of  $\tilde{C}_{DD:KN}$ , respectively. The dotted lines show  $E_{KN}^0$  for the negative parity channel and  $E_{KN}^1$  for the positive parity channel.

difficult task to show that they are related to  $E_{KN}^1$  and  $E_{KN}^2$  given the statistical uncertainties and the available time separation. However, we can check if this gap depends on the spatial size of the lattice. We evaluate this energy gap on our three lattices at  $\kappa_l = 0.153$  and  $\kappa_l = 0.155$  and plot the results in Fig. 14. Within our statistical accuracy the energy gap does not show any strong volume dependence having about the same values of 100 MeV at the two  $\kappa$  values. Within our statistical accuracy the energy gap does not show any strong volume dependence having about the same values of 100 MeV at the two  $\kappa$  values. Although this energy gap agrees with the energy difference between the  $\Theta^+$  and the KN scattering threshold, the mass that we estimate below for the positive channel at the chiral limit is much larger than 1540 MeV to be identified as the  $\Theta^+$ .

Fitting the effective mass derived from  $\Lambda_0(t)$  to Eq. (16) we find, at  $\kappa_l = 0.153$ ,  $E_0^- = 1.228(14)$  for the negative

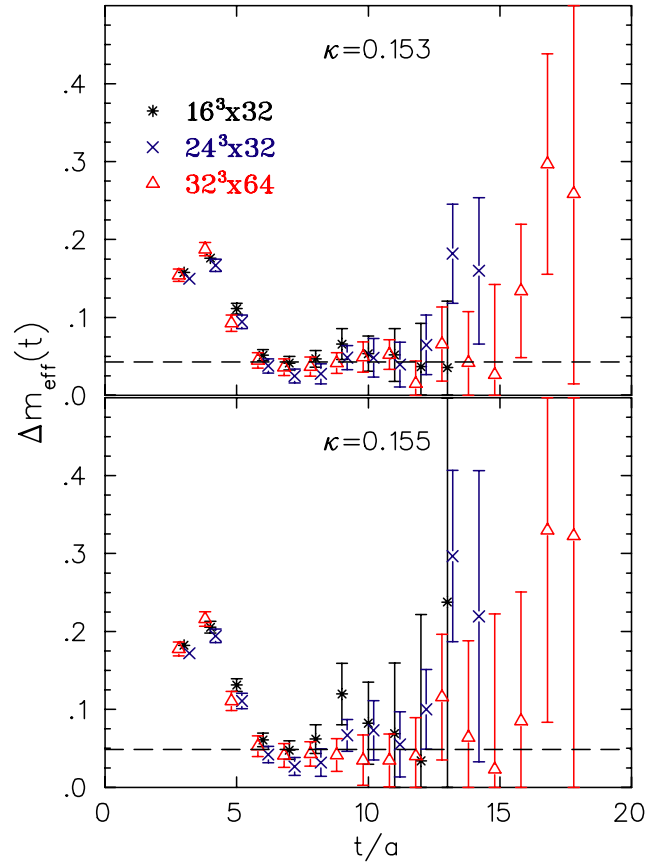


FIG. 14 (color online). The energy gap between the two lowest energy eigenstates as a function of  $t/a$  for the pentaquark in the positive parity channel at  $\kappa_l = 0.153$  (upper graph) and  $\kappa_l = 0.155$  (lower graph) for lattices of size  $16^3 \times 32$  (asterisks),  $24^3 \times 32$  (crosses), and  $32^3 \times 64$  (open triangles). The dashed line shows the plateau value determined on the lattice of size  $16^3 \times 32$ .

parity and  $E_0^+ = 1.438(60)$  for the positive parity channels whereas at  $\kappa_l = 0.155$  we find  $E_0^- = 1.014(20)$  and  $E_0^+ = 1.259(116)$ . These values agree both with those extracted from the local-smeared correlator  $\tilde{C}(t)$  using  $J_{DD}$  and given in Table III and from  $\tilde{\Lambda}_0(t)$  as demonstrated in Fig. 13. The fact that these different ways of constructing the correlation matrices lead to the same value for the energy makes us confident that our results for the lowest state are robust. For the second eigenstate we can only provide an estimate in the positive parity channel. We find that, at our two heaviest pion masses, it is higher in energy by about 100 MeV.

In Fig. 15 we compare the effective masses for the lowest state of the pentaquark system and of the two-pion system. In the two-pion system, as the spatial volume increases, the effective masses start off having higher values because scattering states with higher relative momentum have smaller energy gap at larger spatial volumes, requiring longer time to damp out. Only at large times the ground state dominates the correlator yielding the same

TABLE III. We give, in lattice units, the mass of the pentaquark,  $m^-$  and  $m^+$ , in the negative and positive parity channels, for the lattice of size  $32^3 \times 64$ . They are determined from fitting the effective mass extracted from the local-smear correlator,  $\tilde{C}(t)$ , using  $J_{DD}$  to Eq. (16). The fit range is 5–20 in lattice units and the values at the chiral limit are obtained by linear extrapolation. It has been verified that the values for the masses do not change outside error bars if the lower fit range is increased from 5 to 7–10.

Negative parity		Positive parity
$\kappa_l$	$am^-$	$am^+$
0.153	1.226(17)	1.366 (35)
0.1550	0.999(21)	1.191(45)
0.1554	0.946(23)	1.167(48)
0.1558	0.891(25)	1.149(54)
0.1562	0.834(29)	1.135(63)
$\kappa_c$	0.701(29)	1.036(51)

plateau value on all lattice sizes. In the pentaquark system, on the other hand, the effective masses have the same value in the time interval  $20 < t/a < 30$ . This is the time interval where a resonance is expected to dominate the correlator. However, one has to bear in mind that the statistical errors are bigger than in the two-pion system so that any volume dependence may be harder to detect. This is particularly true in the positive parity channel.

In the following we discuss the scaling of the spectral weights in an attempt to obtain information on the nature of the lowest energy eigenstates. For the same reasons as explained for the two-pion system, we only show the ratio of correlators  $R_{16:24}$ . As can be seen in Fig. 16 for the negative parity channel  $R_{16:24}$  stays close to unity up to time separations  $t/a \sim 20$ . For  $t/a > 20$  where, from our study of the two-pion system, we expect this ratio to start to deviate from unity the errors become large making it difficult to distinguish a single particle state from a scattering state. In the positive channel in this large time window the errors are even larger making this test not applicable. Instead of the ratio  $R_{16:24}$  we plot the spectral weights determined on each volume making a direct comparison to the two-pion system. Again we do this only for the negative parity channel where we have more accurate results. This comparison is shown in Fig. 17 as a function of the lower time range  $t_i/a$  used in the single and double exponential fits to the optimal correlators keeping the upper fit range fixed to 26 for the two smaller lattices and to 56 for the large lattice. For the two-pion system the weights are clearly volume dependent. On the lattice of size  $16^3 \times 32$  the values we obtain, performing a single exponential fit, are independent of the lower fit range for  $t_i/a > 10$  and we can reliably extract the spectral weight of the lowest state. For the  $24^3 \times 32$  lattice the convergence is seen later because suppression of higher momentum states requires larger time separations. For the  $32^3 \times 64$  lattice, the spectral weights are less well determined and can vary

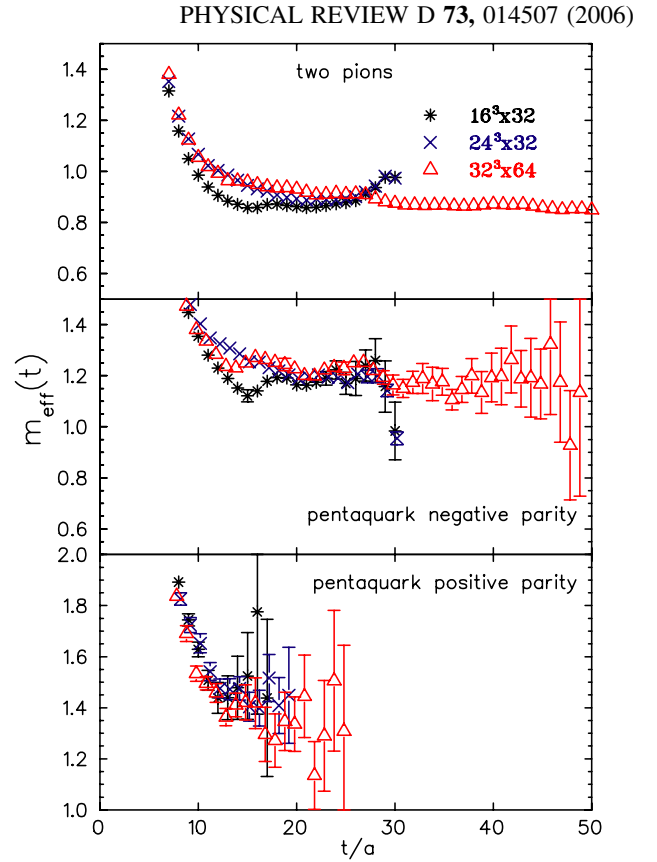


FIG. 15 (color online). The upper graph shows the effective mass for the lowest energy eigenstate of the two-pion system as a function of  $t/a$  at  $\kappa_l = 0.153$ . The middle graph shows the corresponding effective mass for the pentaquark system in the negative parity channel and the lower graph for the pentaquark in the positive parity channel for the lattices of size  $16^3 \times 32$  (asterisks),  $24^3 \times 32$  (crosses), and  $32^3 \times 64$  (open triangles).

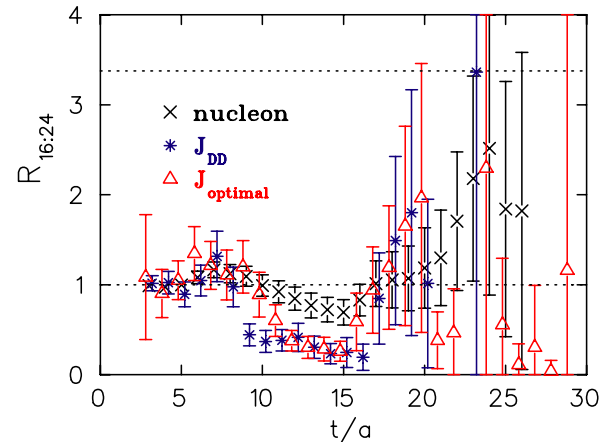


FIG. 16 (color online). The ratio  $R_{16:24}$  versus  $t/a$  for the negative parity channel for the lowest energy eigenstate at  $\kappa_l = 0.153$ . Asterisks show results obtained with correlators using the diquark-diquark interpolating field  $J_{DD}$  and open triangles with  $J_{optimal}$ . For comparison we also show the ratio for the nucleon (crosses). The dotted lines show the expected value of the ratios for a single particle state and a two-particle scattering state.

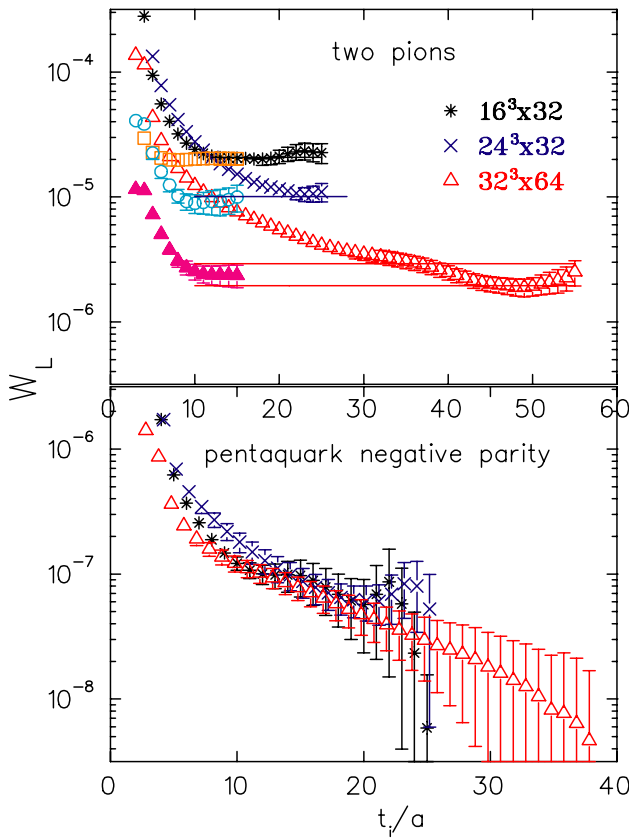


FIG. 17 (color online). We show the spectral weights for the lowest eigenstate at  $\kappa_l = 0.153$  versus the lower fitting range  $t_i/a$  keeping the upper range fixed to 26 for the two smaller lattices and to 56 for the large lattice. The upper graph shows results for the two-pion system and the lower graph for the pentaquark in the negative parity channel for the lattices of size  $16^3 \times 32$  (asterisks for a single exponential fit),  $24^3 \times 32$  (crosses for a single exponential fit), and  $32^3 \times 64$  (open triangles for a single exponential fit). In the case of the two-pion system, we also show results for the weights determined from fitting the correlator to a sum of two exponentials for lattices of size  $16^3 \times 32$  (squares),  $24^3 \times 32$  (circles), and  $32^3 \times 64$  (filled triangles). The solid lines in the upper graph show the plateau values.

by a factor of about 2 depending on which range of  $t_i/a$  we use. However, within this uncertainty, the spectral weight ratio is closer to the values expected for a scattering state than to unity. Fitting to a sum of two exponentials, the spectral weights become independent of the lower fit range for  $t_i/a > 10$  on all three lattices yielding results consistent to those obtained when fitting to a single exponential. This checks that indeed the value we find for the spectral weights does not depend on our fitting scheme. The volume dependence of spectral weights for the pentaquark system

<sup>1</sup>Fitting to a sum of two exponentials yields spectral weights that are consistent with those extracted from the single exponential fit but with errors that are too large to plot in Fig. 17.

is different. The spectral weights extracted from a fit to a single exponential<sup>1</sup> are volume independent for  $10 < t_i/a < 26$ , which is the time range where we can make a comparison. This means that in this range we do not have a single scattering state. The energy gap between the two lowest KN scattering states for  $\kappa_l = 0.153$  is  $a(E_{KN}^1 - E_{KN}^0) = 0.26$  and  $0.13$  on the lattices of size  $16^3 \times 32$  and  $24^3 \times 32$ , respectively, as compared to the energy gap of  $a(2m_\rho - 2m_\pi) = 0.16$  in the two-pion system. This means that, as compared to the two-pion system, the lowest KN scattering state is filtered out at smaller time separations on the smallest lattice and at  $\sim 20\%$  larger times on the  $24^3 \times 32$  lattice. Therefore one would have expected to see a clear volume dependence of the spectral weights on the two smaller lattices which is not observed. On the largest lattice, the fact that the values of the spectral weight decrease as  $t_i/a$  increases beyond 30 is consistent with the expectation that at large time separations a KN s-wave scattering state should dominate. For the positive parity channel extending the upper fit range to large time separations yields statistical errors that are too large to make this test conclusive even at this very heavy pion mass. As the light quark mass decreases the errors on the determination of the spectral weights increase and therefore one would need much larger statistics to reliably extract the weights. Based on the volume study of the spectral weights at  $\kappa_l = 0.153$  we cannot exclude a pentaquark resonance.

Within our variational basis the lowest energy eigenvalue is the only one that we can determine accurately in the negative parity channel. It is shown to be in agreement with the mass extracted from the correlators using either local interpolating fields  $J_{DD}$ ,  $J_{KN}$ , and  $J_{\text{optimal}}$  or the smeared versions of these. Therefore to get an estimate on the light quark mass dependence of the lowest state we use the local-smeared correlators  $\tilde{C}(t)$ . Similarly for the positive parity channel the energy gap between the two lowest energy eigenvalues is about 100 MeV at both  $\kappa = 0.153$  and  $\kappa = 0.155$ . Resolving these two states for smaller quark masses is even harder and therefore we opt to evaluate just the lowest energy which can again be obtained from just using  $\tilde{J}_{DD}$ . This will give us a rough idea of what the chiral limit of this state is. Since the local-smeared correlators are evaluated on our largest volume with antiperiodic b.c. in the time direction, the mass is extracted using the form given in Eq. (16) for which half the time separation is sufficient as demonstrated by the agreement of our results at  $\kappa_l = 0.153$  and  $0.155$ .

The results that we obtain for the mass from the local-smeared correlators for all the light quark masses that we have considered in this work are given in Table III. We note that at  $\kappa_l = 0.155$  diagonalization of the correlation matrix  $\tilde{C}_{DD;KN}(t)$  yields in the negative parity channel  $E_0^- = 1.002(15)$  for the ground state and  $E_1^- = 1.6(2)$  for the first excited state. This value of  $E_0^-$  is in agreement with the

value given in Table III and the value of  $E_1^-$  is in agreement with 1.7(1) extracted from the local-smearred correlator via Eq. (16). The pentaquark masses at the chiral limit given in Table III are obtained by linearly extrapolating the results determined on the set of five  $\kappa_l$  values using Eq. (13). The corresponding results for the kaon and nucleon masses at the chiral limit are given in Table I. We show all chiral extrapolations in Fig. 18. Note that the slope in the case of pentaquarks is steeper than for the nucleon or the kaon which means that the mass gap between pentaquarks and KN increases with the quark mass, giving at  $\kappa_l = 0.153$  a gap of about 170 MeV as mentioned earlier. From the values obtained at the chiral limit, we can evaluate the ratios of the mass of the candidate pentaquark in the positive and negative parity channels to the mass of the kaon-nucleon system,  $m_{KN}$ . The values that we find for these ratios are  $1.12 \pm 0.04$  for the negative parity and  $1.65 \pm 0.09$  for the positive. Substituting the physical kaon and nucleon mass values leads to the determination of the mass in physical units. We find in the negative and positive parity channels the values

$$m^- = 1.605 \pm 0.058 \text{ GeV} \quad m^+ = 2.36 \pm 0.13 \text{ GeV}, \quad (22)$$

respectively. As we have already pointed out, the ratio between the mass of the  $\phi$  meson evaluated at  $\kappa_s = 0.155$  and the mass of the nucleon at the chiral limit is  $1.002 \pm 0.025$ , within 10% of the value of 1.087 obtained using the physical  $\phi$  meson and nucleon masses. Similarly the ratio  $m_K/m_N = 0.493(17)$  at the chiral limit is very close to the physical value of 0.526.

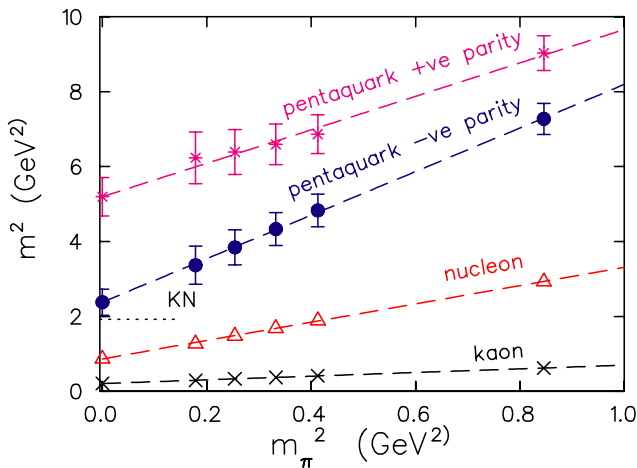


FIG. 18 (color online). The mass squared of the kaon (crosses), nucleon (open triangles), pentaquark in the negative parity channel (filled circles), and in the positive parity channel (asterisks) plotted versus the pion mass squared. We use the nucleon mass at the chiral limit to set the scale obtaining  $a^{-1} = 2.2 \text{ GeV}$ . The dashed lines show the linear extrapolations to the chiral limit. The dotted line shows the KN threshold at the chiral limit.

Finally we compare our analysis to other lattice studies of the pentaquark system. All lattice studies so far are carried out in quenched QCD. The first pioneering studies with Wilson fermions were carried out by Csikor *et al.* [12] using a variant of the KN-interpolating field,  $J'_{KN}$ , where the color index of the  $\bar{s}$  is coupled to a light quark in the nucleon instead of in the kaon, and Sasaki [13] using the diquark-diquark interpolating field. Both found evidence for a pentaquark state. Motivated by these studies we looked at the pentaquark density-density correlator in order to learn about the internal structure of the  $\Theta^+$  [15]. Chiu and Hsieh [14] using overlap fermions performed a variational analysis using interpolating fields  $J_{KN}$ ,  $J'_{KN}$ , and  $J_{DD}$ . Their conclusion was that there is a resonance in the positive parity channel, which in the chiral limit has a mass close to that of the  $\Theta^+$  (1540). The next lattice group to have results on the pentaquark system was Mathur *et al.* [17]. They used interpolating fields  $J_{KN}$  and  $J'_{KN}$  [12]. By studying the scaling of spectral weights on two volumes of size  $12^3 \times 28$  and  $16^3 \times 28$  using a sequential Bayesian method, they concluded that the states that they observed were KN scattering states. In the work of Ishii *et al.*, in addition to periodic boundary conditions, antiperiodic boundary conditions were used in the spatial direction for the light quarks. With antiperiodic boundary conditions the lowest momentum allowed for each quark is  $\pi/L$ . Therefore in the negative parity channel switching from periodic to antiperiodic b.c. should increase the energy of the lowest KN scattering state. They indeed observed the expected shift in energy concluding that the lowest state is a KN scattering state. Our analysis is closest to the analysis carried out in Ref. [16]. Diagonalizing the  $2 \times 2$  correla-

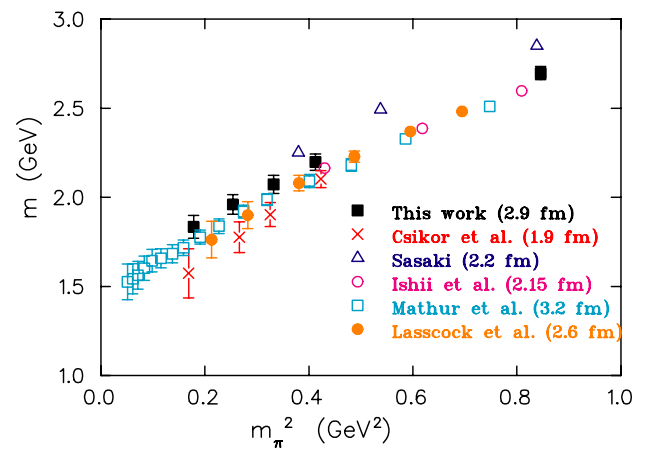


FIG. 19 (color online). The mass of the lowest eigenstate of the pentaquark system in the negative parity channel as a function of the pion mass squared. Filled squares show the results of this work, crosses are data from Ref. [12], open triangles from Ref. [13], open circles from Ref. [18], open squares from Ref. [17], and filled circles from Ref. [19]. In each case we give the spatial length of the lattice.

tion matrix constructed using  $J_{KN}$  and  $J'_{KN}$ , and using a large number of configurations, they were able to accurately determine the two lowest eigenvalues in the negative parity channel and check scaling of their spectral weights. Based on this scaling they concluded that the lowest state is the s-wave KN scattering state whereas the second is a resonance state that they identified as the  $\Theta^+$ . In the positive parity channel, they obtained only one state, which they concluded is not the p-wave KN scattering state. Finally, after the completion of our work a study of the binding energy in the pentaquark system as a function of the light quark mass was carried out in Ref. [19]. The fact that they saw no increase in the binding as the light quark mass decreases led them to conclude that there is no pentaquark resonance. Following Ref. [19], we compare our results given in Table III for the negative parity channel to the results from other lattice groups in Fig. 19. The small variations in the extracted values for the mass among different groups can be attributed, at least partly, to small differences in the strange quark mass. Also, errors due to the choice of the lattice scale  $a$  are not included.

#### IV. CONCLUSIONS

We have presented a computation of the mass of the pentaquark system using interpolating fields, which are motivated by the diquark-diquark and diquark-triquark structure proposed for the  $\Theta^+$  in order to explain its narrow width. Despite the difference in the structure of these interpolating fields, the values obtained for the lowest mass of the pentaquark system using either interpolating field are in agreement with each other. They are also in agreement with the lowest energy eigenvalue determined from the analysis of the correlation matrices constructed using either local or smeared KN and diquark-diquark interpolating fields as a basis. A study of the two-pion system in the  $I = 2$  channel where no low lying resonances are present is carried out to check our lattice techniques. By analyzing the correlation matrix constructed using products of pion and rho-meson interpolating fields, we accurately determined that the two lowest states are the s-wave two-pion and two-rho scattering states with a mass gap which is about 320 MeV at a quark mass that corresponds to pion mass of about 830 MeV. It is explicitly verified that these are s-wave states by projecting to zero relative momentum on our smallest lattice. We note that the energies obtained by diagonalizing the correlation matrix in the center of mass frame are a mixture of scattering states of different relative momentum even when the two lowest states are scattering states and only at large time separations they yield the correct ground state. This is a relevant result since in many lattice studies it is assumed that a similar diagonalization resolves the scattering states with different relative momentum. By studying the spectral weights for the two lowest eigenstates in the two-pion

system on our three lattice volumes, we show that the correct scaling with the spatial volume sets in at large times requiring accurate determination of local correlators. The spectral weights in the pentaquark system show no volume dependence in the time range where in the two-pion system a clear scaling of spectral weights is seen. Therefore based on our spectral weights results we cannot exclude a resonance pentaquark state. In the negative parity channel our correlation matrix analysis gives accurately one state close to the KN threshold. The first excited state in this channel is very poorly determined. We would like to stress that the fact that within the time extent of our smaller lattices the spectral weights do not scale with the volume only leads to the conclusion that we do not have a single scattering state. Given the fact that within our statistics and time ranges we are unable to accurately resolve a lower KN- scattering state and a higher close-by single particle state does not permit us to draw any definite conclusion regarding the existence of the  $\Theta^+$ . However, we have shown in this work that one would need very accurate data, better interpolating fields, and lattices with large time extension in order to reliably resolve the low lying states and perform a spectral weights analysis to exclude or show the existence of the  $\Theta^+$ . Using the fact that the lowest eigenstate from the correlation matrix analysis yields an energy in agreement with that extracted with  $J_{DD}$  allows us to use the local-smeared diquark-diquark interpolating field to compute the mass of this state. This is carried out on a set of five values of light quark masses on our large lattice. A linear extrapolation to the chiral limit leads to a value for the mass which is about 10% above the KN threshold. In the positive parity channel the two lowest eigenstates are separated by an energy gap of about 100 MeV at the two heaviest pion masses. However, the mass that we find in the chiral limit, determined in the same way as in the negative parity channel, is about 900 MeV above the KN threshold and therefore too high to be identified with the  $\Theta^+(1540)$ . In summary, we have shown that, within this analysis in quenched lattice QCD and using Wilson fermions, we cannot exclude a pentaquark state, which in the negative parity channel has a mass about 750 MeV lower than in the positive channel. However, with the lattice sizes used and within our statistics, the existence of the  $\Theta^+$  has also not been established from this study. In order to reach a definite conclusion regarding its existence, one would require a more detail and accurate computation involving a larger and better basis of interpolating fields, lattices with larger temporal extent and more statistics.

#### ACKNOWLEDGMENTS

A. Tsapalis acknowledges funding from the Leventis Foundation. This work has been supported in part by the EU Integrated Infrastructure Initiative Hadron Physics (I3HP) under Contract No. RII3-CT-2004-506078.

- [1] T. Nakano *et al.* (LEPS Collaboration), Phys. Rev. Lett. **91**, 012002 (2003).
- [2] V.V. Barmin *et al.* (DIANA Collaboration), Phys. At. Nucl. **66**, 1715 (2003); S. Stepanyan *et al.* (CLAS Collaboration), Phys. Rev. Lett. **91**, 252001 (2003); J. Barth *et al.* (SAPHIR Collaboration), Phys. Lett. B **572**, 127 (2003).
- [3] A. E. Asratyan, A. G. Dolgolenko, and M. A. Kubantsev, Phys. At. Nucl. **67**, 682 (2004); V. Kubarovsky *et al.* (CLAS Collaboration), Phys. Rev. Lett. **92**, 032001 (2004); A. Airapetian *et al.* (HERMES Collaboration), Phys. Lett. B **585**, 213 (2004); S. Chekanov *et al.* (ZEUS Collaboration), Phys. Lett. B **591**, 7 (2004); M. Abdel-Barv *et al.* (COSY-TOF Collaboration), Phys. Lett. B **595**, 127 (2004); A. Aleev *et al.* (SVD Collaboration), Phys. At. Nucl. **68**, 974 (2005).
- [4] J.Z. Bai *et al.* (BES Collaboration), Phys. Rev. D **70**, 012004 (2004); B. Aubert *et al.* (BABAR Collaboration), hep-ex/0408064; K. Abe *et al.* (Belle Collaboration), hep-ex/0411005; S. R. Armstrong, Nucl. Phys. B, Proc. Suppl. **142**, 364 (2005); S. Schael *et al.* (ALEPH Collaboration), Phys. Lett. B **599**, 1 (2004); I. Abt *et al.* (HERA-B Collaboration), Phys. Rev. Lett. **93**, 212003 (2004); Yu.M. Antipov *et al.* (SPHINX Collaboration), Eur. Phys. J. **21**, 455 (2004); M.J. Longo *et al.* (HyperCP Collaboration), Phys. Rev. D **70**, 111101 (2004); D. O. Litvintsev (CDF Collaboration), Nucl. Phys. B, Proc. Suppl. **142**, 374 (2005); K. Stenson *et al.* (FOCUS Collaboration), Int. J. Mod. Phys. A **20**, 3745 (2005); R. Mizuk *et al.* (Belle Collaboration), hep-ex/0411005; C. Pinkerton *et al.* (PHENIX Collaboration), J. Phys. G **30**, S1201 (2004).
- [5] After the submission of this work to Phys. Rev. D, the CLAS collaboration has reported a negative result, M. Battaglier *et al.*, hep-ex/0510061.
- [6] D. Diakonov, V. Petrov, and M. Polyakov, Z. Phys. A **359**, 305 (1997).
- [7] A. Casher and S. Nussinov, Phys. Lett. B **578**, 124 (2004).
- [8] M. Karliner and H.J. Lipkin, Phys. Lett. B **575**, 249 (2003).
- [9] X.-C. Song and S.-L. Zhu, Mod. Phys. Lett. A **19**, 2791 (2004).
- [10] C. Alexandrou and G. Koutsou, Phys. Rev. D **71**, 014504 (2005).
- [11] R. Jaffe and F. Wilczek, Phys. Rev. Lett. **91**, 232003 (2003).
- [12] F. Csikor, Z. Fodor, S. D. Katz, and T. G. Kovacs, J. High Energy Phys. **11** (2003) 070.
- [13] S. Sasaki, Phys. Rev. Lett. **93**, 152001 (2004).
- [14] T.-W. Chiu and T.-H. Hsieh, Phys. Rev. D **72**, 034505 (2005).
- [15] C. Alexandrou, G. Koutsou, and A. Tsapalis, Nucl. Phys. B, Proc. Suppl. **140**, 275 (2005).
- [16] T. T. Takahashi, T. Umeda, T. Onogi, and T. Kunihiro, hep-lat/0410025.
- [17] N. Mathur *et al.*, Phys. Rev. D **70**, 074508 (2004).
- [18] N. Ishii *et al.*, Phys. Rev. D **71**, 034001 (2005).
- [19] B. G. Lasscock *et al.*, Phys. Rev. D **72**, 014502 (2005).
- [20] S. Sasaki, Nucl. Phys. B, Proc. Suppl. **140**, 127 (2005); G. Fleming, hep-lat/050101.
- [21] F. Okiharu, H. Suganuma, and T. T. Takahashi, hep-lat/0410021.
- [22] M. Lüscher, Nucl. Phys. **B364**, 237 (1991).
- [23] S. Sasaki, T. Blum, and S. Ohta, Phys. Rev. D **65**, 074503 (2002).
- [24] S. Güsken, Nucl. Phys. Proc. Suppl. **17**, 361 (1990); C. Alexandrou *et al.* Nucl. Phys. **B414**, 815 (1994).
- [25] N. A. Campbell, A. Huntley, and C. Michael, Nucl. Phys. **B306**, 51 (1988); M. Lüscher and U. Wolff, Nucl. Phys. **B339**, 222 (1990); M. Guagnelli, R. Sommer, and H. Wittig, Nucl. Phys. **B535**, 389 (1998).
- [26] D. Leinweber, R. M. Woloshyn, and T. Draper, Phys. Rev. D **43**, 1659 (1991).
- [27] NERSC archive, G. Kilcup *et al.*, Nucl. Phys. B, Proc. Suppl. **53**, 345 (1997).
- [28] M. Lüscher, Nucl. Phys. **B354**, 531 (1991).